

1-1-2014

# Site-Directed Mutagenesis Of Conserved Amino Acids Residues In N5-Carboxyaminoimidazole Ribonucleotide Mutase: Converting N5-Cair Mutase Into Aminoimidazole Ribonnucleotide Carboxylase & Developing A High-Throughput Screening Assay For The Discovery Of N5-Carboxyaminoimidazole Ribonucleotide Mutase

Zhiwen Shi  
*Wayne State University,*

Follow this and additional works at: [http://digitalcommons.wayne.edu/oa\\_theses](http://digitalcommons.wayne.edu/oa_theses)

 Part of the [Medicinal Chemistry and Pharmaceutics Commons](#)

---

## Recommended Citation

Shi, Zhiwen, "Site-Directed Mutagenesis Of Conserved Amino Acids Residues In N5-Carboxyaminoimidazole Ribonucleotide Mutase: Converting N5-Cair Mutase Into Aminoimidazole Ribonnucleotide Carboxylase & Developing A High-Throughput Screening Assay For The Discovery Of N5-Carboxyaminoimidazole Ribonucleotide Mutase" (2014). *Wayne State University Theses*. Paper 354.

**Site-Directed Mutagenesis of Conserved Amino Acids Residues in N<sup>5</sup>-  
Carboxyaminoimidazole Ribonucleotide Mutase: converting N<sup>5</sup>-CAIR  
mutase into Aminoimidazole Ribonnucleotide carboxylase  
&  
Developing a High-Throughput Screening Assay for the Discovery of N<sup>5</sup>-  
Carboxyaminoimidazole Ribonucleotide Mutase Inhibitors**

by

**ZHIWEN SHI**

**THESIS**

Submitted to the Graduate School

of Wayne State University,

Detroit, Michigan

in partial fulfillment of the requirements

for the degree of

**MASTERS OF SCIENCE**

2014

MAJOR: PHARMACEUTICAL SCIENCES

Approved by:

---

Advisor

Date

**© COPYRIGHT BY**

**Zhiwen Shi**

**2014**

**All Rights Reserved**

## **DEDICATION**

To my parents and friends

## **ACKNOWLEDGMENTS**

I want thank many people for helping me to complete my master degree. First, I would like thank my advisor Dr. Steven Firestine, who gave me a lot help during the past two years and allowed me to do man stupid things. I also want to thank my lab mates, Dr. Shiv Sharma, Cale Streeter, Qian Lin and Mingyang Zhao, who helped me to solve many problems in the lab.

I would like to thank my committee members Dr. Timothy Stemmler and Dr. Ladislau Kovari who provided many useful suggestions for my thesis.

I also want to thank Dr. Hirata and Aiko who helped to make all the mutants plasmids for my projects. And I want to thank Dr. Olivia Merkel and Yuran Xie who help me to use the RT-PCR.

Finally, I want to thank Pharmaceutical Science department who offered me the opportunity to study here.

## TABLE OF CONTENTS

DEDICATION .....	ii
ACKNOWLEDGMENTS .....	iii
LIST OF TABLES .....	vii
LIST OF FIGURES .....	viii
LIST OF SCHEMES .....	ix
Chapter 1. Site-Directed Mutagenesis of Conserved Amino Acids Residues in N <sup>5</sup> -Carboxyaminoimidazole Ribonucleotide Mutase: converting N <sup>5</sup> -CAIR into Aminoimidazole Ribonucleotide carboxylase.....	1
1.1. Introduction .....	1
1.1.1. The role of purine nucleotides in cellular activity .....	1
1.1.2. Salvage pathway.....	1
1.1.3. <i>De novo</i> purine biosynthetic pathway .....	2
1.1.4. PurK.....	5
1.1.5. N <sup>5</sup> -CAIR .....	5
1.1.6. Class I and Class II PurEs .....	5
1.1.6.1. AIR is the substrate of Class II PurEs but not Class I PurEs.....	6
1.1.6.2. N <sup>5</sup> -CAIR is the substrate of Class I PurE but not Class II PurE.....	6
1.1.7. Sequence and structural studies.....	8
1.2. Results .....	11

1.2.1.	Enzyme expression and purification .....	11
1.2.2.	Protein folding of mutants .....	12
1.2.2.1.	Limited proteolysis for WT and mutant PurEs.....	12
1.2.2.2.	Circular dichroism spectrum for folding of mutants.....	14
1.2.3.	Steady-State kinetic analysis of the PurE mutants.....	15
1.2.4.	Comparison of the CO <sub>2</sub> dependence of wild type PurE, human AIR carboxylases and mutant PurE.....	16
1.2.5.	The PurC-coupled assay.....	20
1.3.	Discussion.....	23
1.3.1.	Possible mechanism the conversion of N <sup>5</sup> -CAIR to CAIR.....	25
1.3.2.	What role does His71 play in this mechanism?.....	25
1.3.3.	The open channel hypothesis for AIR carboxylase.....	27
1.4.	Future Studies.....	28
Chapter 2. Developing a High-Throughput Screening Assay for the Discovery of N <sup>5</sup> -Carboxyaminoimidazole Ribonucleotide Mutase Inhibitors.....		29
2.1.	Introduction .....	29
2.1.1.	Drug Resistance and new antibiotics .....	29
2.1.2.	PurE as a new target for antibiotic drug discovery... ..	29
2.1.3.	High-throughput screening.....	29

2.1.4.	Limitation of CAIR decarboxylase assay.....	30
2.2.	Results and discussion.....	31
2.2.1.	AIR carboxylation assay.....	31
2.2.2.	Thermoflour®.....	32
2.2.3.	Metal stopping assay .....	35
2.2.3.1.	Assay design and hypothesis .....	35
2.2.3.2.	Experiments and results .....	38
Chapter 3	Materials and Methods.....	40
3.1	Materials.....	40
3.2	Expression and purification of WT and mutated PurEs .....	40
3.3	Limited Proteolysis .....	42
3.4	Circular Dichroism.....	42
3.5	Steady-state kinetic.....	42
3.6	CO <sub>2</sub> -dependence assay .....	43
3.7	PurC coupled assay. ....	43
3.8	Thermoflour® .....	43
3.9	Metal stopping assay.....	44
REFERENCE	.....	45
ABSTRACT	.....	53
AUTOBIOGRAPHICAL STATEMENT	.....	55



## LIST OF TABLES

Table 1. Enzymes in de novo purine biosynthetic pathway. ....	4
Table 2. Abbreviation of substrates .....	4
Table 3 Steady-State Kinetic Constants for Wild-type PurE and Mutants.....	15

## LIST OF FIGURES

Figure 1. The de novo purine biosynthetic pathway.....	3
Figure 2 Crystal structure of Class I and Class II PurEs structures. ....	7
Figure 3. Sequence alignments between Class I and Class II PurEs. ....	8
Figure 4. SDS-PAGE of limited proteolysis .....	13
Figure 5. Far-UV CD spectra of H71G and Wild Type PurE .....	14
Figure 6. AIR incubated with WT or mutants PurE in the presence of CO <sub>2</sub> . ....	17
Figure 7. Comparaison of WT and mutant PurEs with CO <sub>2</sub> or HCO <sub>3</sub> <sup>-</sup> . ....	18
Figure 8 Mutation H71G with one-carbonate substrates incubated with 1 µg carbonic anhydrase. ....	19
Figure 9 PurC coupled assay .....	21
Figure 10 PurC coupled assay to monitor N5-CAIR turnover. ....	21
Figure 11. Dimer structure of WT Class I PurE.....	26
Figure 12 Procedure of PurC coupled assay.....	31
Figure 13 Fluorescence intensity versus temperature for unfolding PurEs in the presence of SYPRO orange. ....	32
Figure 14 The melting temperature versus the concentration of compounds. .	33
Figure 15. Zn <sup>2+</sup> stops PurE from converting CAIR to AIR. ....	36
Figure 16. Fluorescent signal scan for Zinc, AIR and CAIR. ....	36
Figure 17. Wavelength versus fluorescence.....	37
Figure 18. CAIR concentration versus Fluorescence.....	37
Figure 19 Fluorescent signal scan with PurEs.....	38

## LIST OF SCHEMES

Scheme 1 Salvage pathway .....	2
Scheme 2 Simple mechanistic model for Class I and Class II PurEs .....	25
Scheme 3 Transfer model of CO <sub>2</sub> from N5-CAIR to AIR .....	27

## Chapter 1.

### Site-Directed Mutagenesis of Conserved Amino Acids Residues in N<sup>5</sup>-Carboxyaminoimidazole Ribonucleotide Mutase: converting N<sup>5</sup>-CAIR into Aminoimidazole Ribonucleotide carboxylase

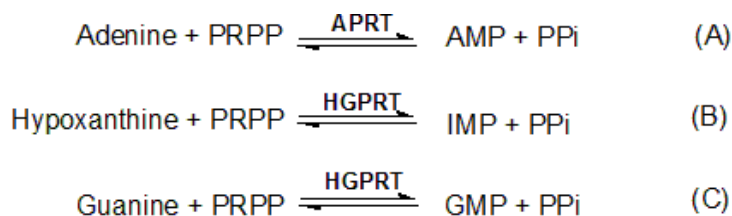
#### 1.1. Introduction

##### 1.1.1. The role of purine nucleotides in cellular activity

Purine nucleotides play an important cellular role. They are utilized in energy storage (ATP), the synthesis of cofactors (NADH, B-12) and in the synthesis of amino acids and secondary natural products. Given the importance of purines to the cell, it is not surprising that two pathways exist for their synthesis, namely the salvage and *de novo* biosynthetic pathways.<sup>1,2</sup>

##### 1.1.2. Salvage pathway

The salvage pathway is a “recycle” pathway, where free bases generated from the degradation of nucleic acids are used to prepare new nucleotides through multiple enzymes. There are two critical enzymes which are commonly used. Adenine phosphoribosyltransferase (APRT) catalyzes the attack of free adenine onto 5-phosphoribosyl- $\alpha$ -pyrophosphate (PRPP) to yield AMP and PP<sub>i</sub> (**Scheme 1 Salvage pathway A**). The other enzyme is hypoxanthine-guanine phosphoribosyltransferase (HGPRT) which catalyzes a similar reaction to transfer guanine to PRPP to generate GMP (**Scheme 1 Salvage pathway C**). This enzyme also catalyzes the reaction of hypoxanthine with PRPP to give IMP (**Scheme 1 Salvage pathway B**).<sup>3</sup>

**Scheme 1 Salvage pathway**

The amount of purine nucleotides prepared by the salvage pathway is about 1%, so the pathway is utilized predominately for cellular stasis. For cells undergoing division, new purine nucleotides must be created. They are synthesized from the *de novo* purine biosynthetic pathway.<sup>4</sup>

**1.1.3. *De novo* purine biosynthetic pathway**

Unlike the salvage pathway, the *de novo* purine pathway synthesizes the purine heterocycle from basic building blocks (**Figure 1**). In this pathway, PRPP is the starting substrate that is ultimately converted to IMP. The pathway is intriguing because of the interesting chemistry which occurs in the pathway and also because it is one of the few primary metabolic pathway which is different between microbes and humans.<sup>5</sup> The difference is focused on the conversion of aminoimidazole ribonucleotides (AIR) to 4-carboxy-5-aminoimidazole ribonucleotide (CAIR). In humans, AIR is directly converted to CAIR by the enzyme AIR carboxylase (Class II PurE), requiring CO<sub>2</sub> as the one carbon substrate. In most bacteria, two steps and two enzymes are needed to convert AIR to CAIR. Step one is catalyzed by N<sup>5</sup>-carboxyaminoimidazole ribonucleotide (N<sup>5</sup>-CAIR) synthetase (PurK) which converts AIR to N<sup>5</sup>-CAIR

with support of ATP and  $\text{HCO}_3^-$ . The second step is the conversion of  $\text{N}^5$ -CAIR to CAIR catalyzed by  $\text{N}^5$ -CAIR mutase (Class I PurE).<sup>6,7</sup>

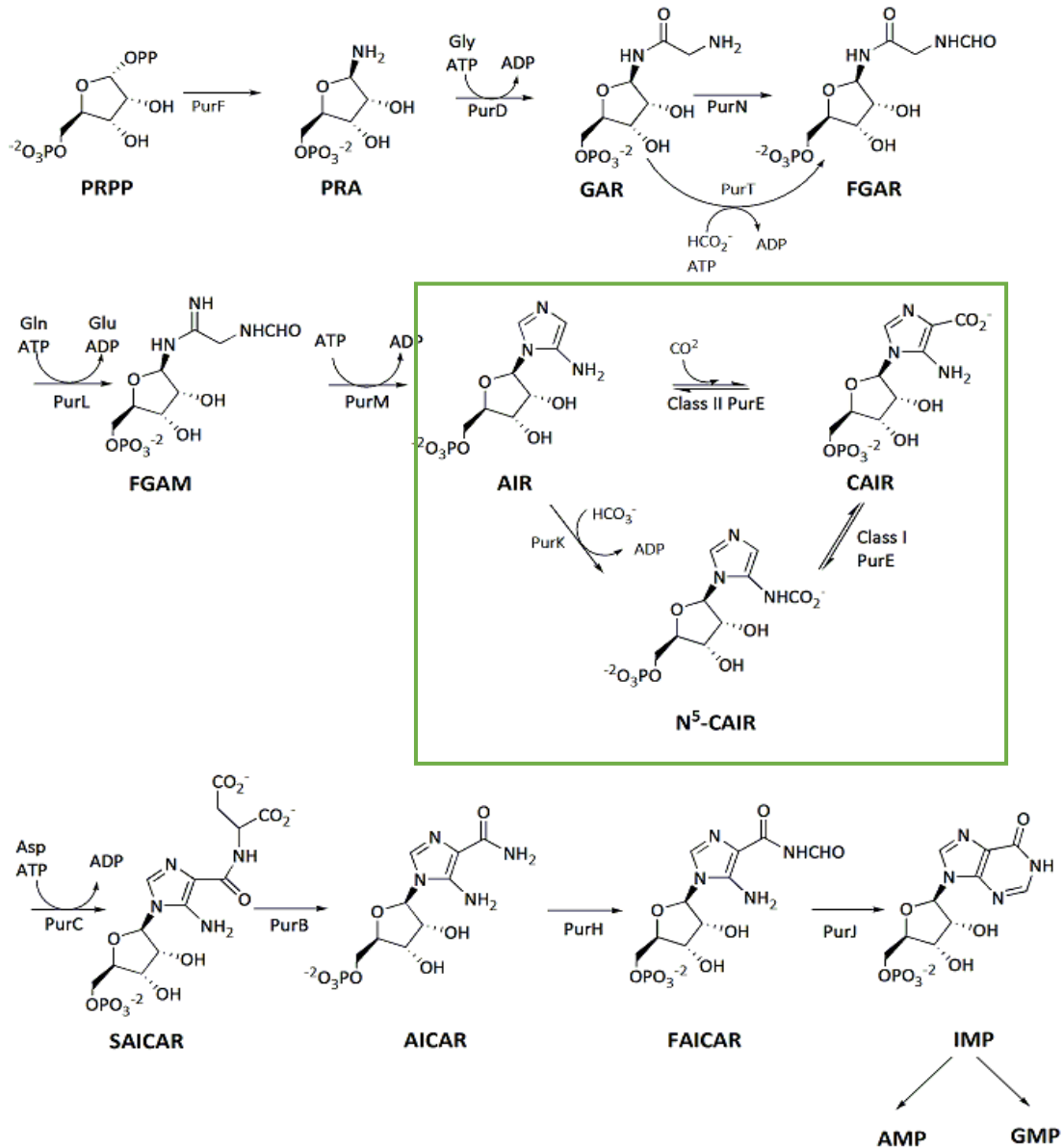


**Figure 1. The *de novo* purine biosynthetic pathway. The green square highlights the difference between Class I and Class II PurEs found in microbes versus higher eukaryotes. The enzyme names and abbreviations of substrates can be found in Tables 1 and 2**

**Table 1. Enzymes in de novo purine biosynthetic pathway.**

<b>Gene</b>	<b>Enzyme name</b>
<b>PurF</b>	PRPP amidotransferase
<b>PurD</b>	GAR synthetase
<b>PurN</b>	GAR transformylase
<b>PurT</b>	FGAR synthetase
<b>PurL</b>	FGAM synthetase
<b>PurM</b>	AIR synthetase
<b>Class II PurE</b>	AIR carboxylase
<b>PurK</b>	N <sup>5</sup> -CAIR synthetase
<b>Class I PurE</b>	N <sup>5</sup> -CAIR mutase
<b>PurC</b>	SAICAR synthetase
<b>PurB</b>	Adenylosuccinate lyase
<b>PurH</b>	AICAR transformylase
<b>PurJ</b>	IMP cyclohydrolase

**Table 2. Abbreviation of substrates**

<b>Abbreviation of intermediate</b>	<b>Full Name</b>
<b>PRPP</b>	5-Phosphoribosyl- $\alpha$ -pyrophosphate
<b>PRA</b>	5-Phosphoribosylamine
<b>GAR</b>	Glycineamide ribonucleotide
<b>FGAR</b>	N-formylglycineamide ribonucleotide
<b>FARM</b>	N-formylglycineamidine ribonucleotide
<b>AIR</b>	Aminoimidazole ribonucleotide
<b>N<sup>5</sup>-CAIR</b>	N <sup>5</sup> -Carboxyaminoimidazole ribonucleotide
<b>CAIR</b>	4-Carboxy-5-aminoimidazole ribonucleotide
<b>SAICAR</b>	Succino 5-aminoimidazole-4-carboxamide ribonucleotide
<b>AICAR</b>	Aminoimidazole-4-carboxamide ribonucleotide
<b>FAICAR</b>	5-Formamido-4-imidazolecarboxamide ribonucleotide
<b>IMP</b>	Inosine monophosphate

#### **1.1.4. PurK**

PurK is one of the ATP-grasp enzymes and its active site includes ATP, AIR and bicarbonate subsites.<sup>8</sup> As mentioned above, PurK catalyzes the turnover of AIR to N<sup>5</sup>-CAIR. This is an ATP-dependent process and links CO<sub>2</sub> to the N5 amino group on AIR to generate N<sup>5</sup>-CAIR. However, PurK is not required under the condition of high CO<sub>2</sub> concentration as AIR can be non-enzymatically converted to N<sup>5</sup>-CAIR without the support of ATP.<sup>9</sup>

#### **1.1.5. N<sup>5</sup>-CAIR**

N<sup>5</sup>-CAIR had not been known as an intermediate in the pathway until the 1990s. This is likely due to the fact that it is a highly unstable compound. It is sensitive to pH and temperature. At 30 °C and pH 7.8, the half-life of N<sup>5</sup>-CAIR is about 0.9 minutes, where it ready breaks down to AIR.<sup>10</sup> The low stability has important implication for how bacteria handle this metabolic intermediate in the middle of a biosynthetic pathway.

#### **1.1.6. Class I and Class II PurEs**

Previous studies have shown that the Class I and Class II PurEs are evolutionarily related to each other. Each catalyzes a reversible reaction to generate the same product, CAIR. In addition, both have extremely similar protein structures (**Figure 2**), and shared about 20-30% sequence identity with each other.<sup>11</sup> Despite these similarities, there exist critical differences between these two classes of PurEs.



**1.1.6.1. AIR is the substrate of Class II PurEs but not Class I PurEs**

When AIR is incubated with Class II PurEs in the presence of CO<sub>2</sub>, rapid CAIR formation is observed.<sup>12</sup> In contrast, addition of N<sup>5</sup>-CAIR or PurK (to produce N<sup>5</sup>-CAIR in situ) fail to give a burst of CAIR formation.<sup>9</sup> NMR studies on the conversion of CAIR by the Class II PurEs fail to detect any N<sup>5</sup>-CAIR and instead yield AIR.<sup>13</sup>

**1.1.6.2. N<sup>5</sup>-CAIR is the substrate of Class I PurE but not Class II PurE**

NMR spectroscopy was applied to investigate and analyze the reverse reaction of CAIR with Class I PurE. NMR analysis showed that CAIR is first converted into N<sup>5</sup>-CAIR which is then non-enzymatically converted to AIR.<sup>10</sup> This is a strong evidence that Class I PurE catalyzes N<sup>5</sup>-CAIR rather than AIR to form CAIR. Addition of CO<sub>2</sub> to AIR and Class I PurE gives a decrease in absorbance (due to N<sup>5</sup>-CAIR formation) followed by an increase in absorbance due to CAIR formation. This study indicates that N<sup>5</sup>-CAIR, not AIR and CO<sub>2</sub>, are substrates for Class I PurEs.<sup>13</sup>

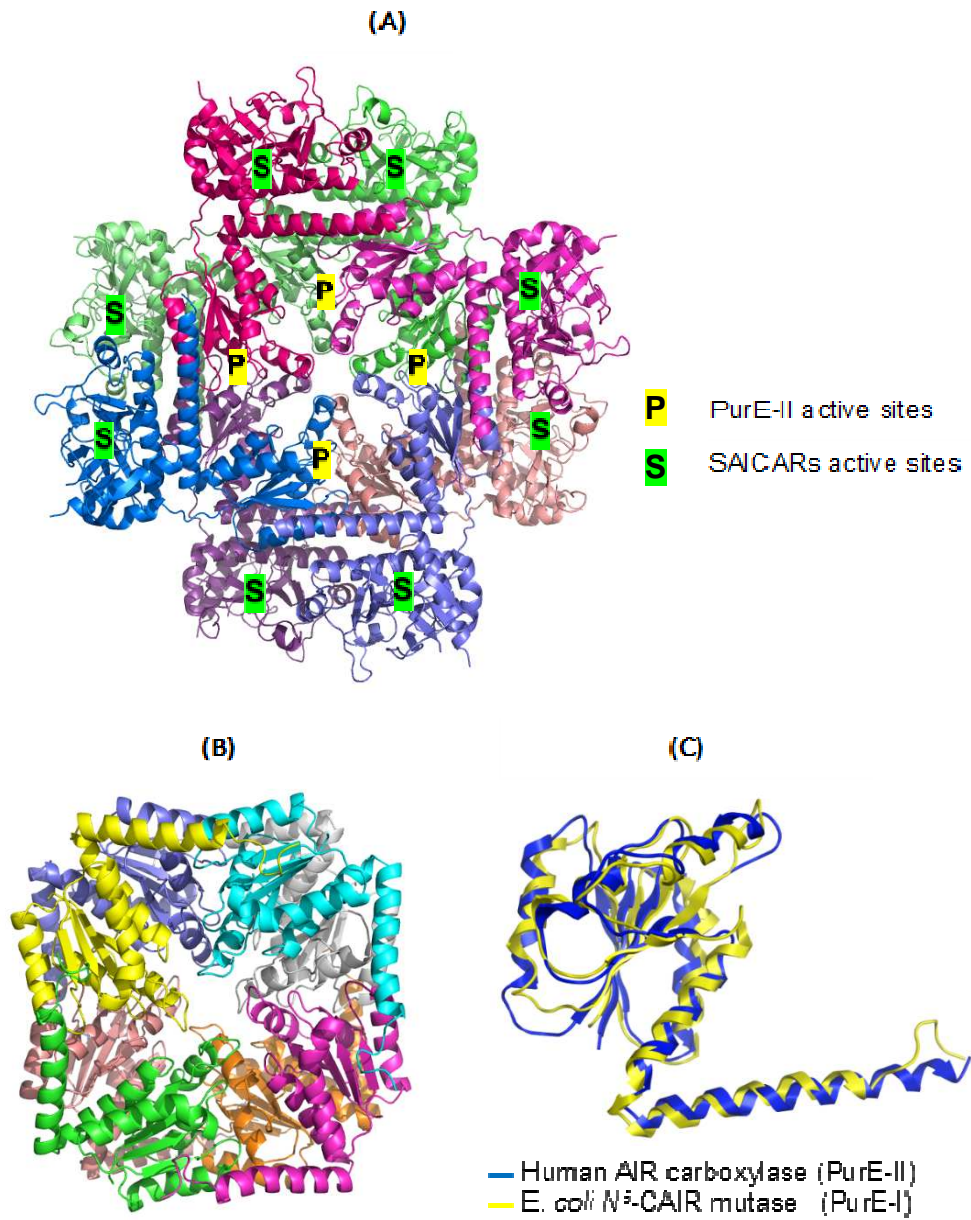


**Figure 2** Crystal structure of Class I and Class II PurEs structures. (A) Human PAICS (PDB 2H31) contains Class II PurE active sites and SAICAR synthetase active sites; (B) *E. coli* PurE (PDB 2ATE). (C) Superposed monomer structures of Class I (yellow) Class II (blue) PurE

### 1.1.7. Sequence and structural studies

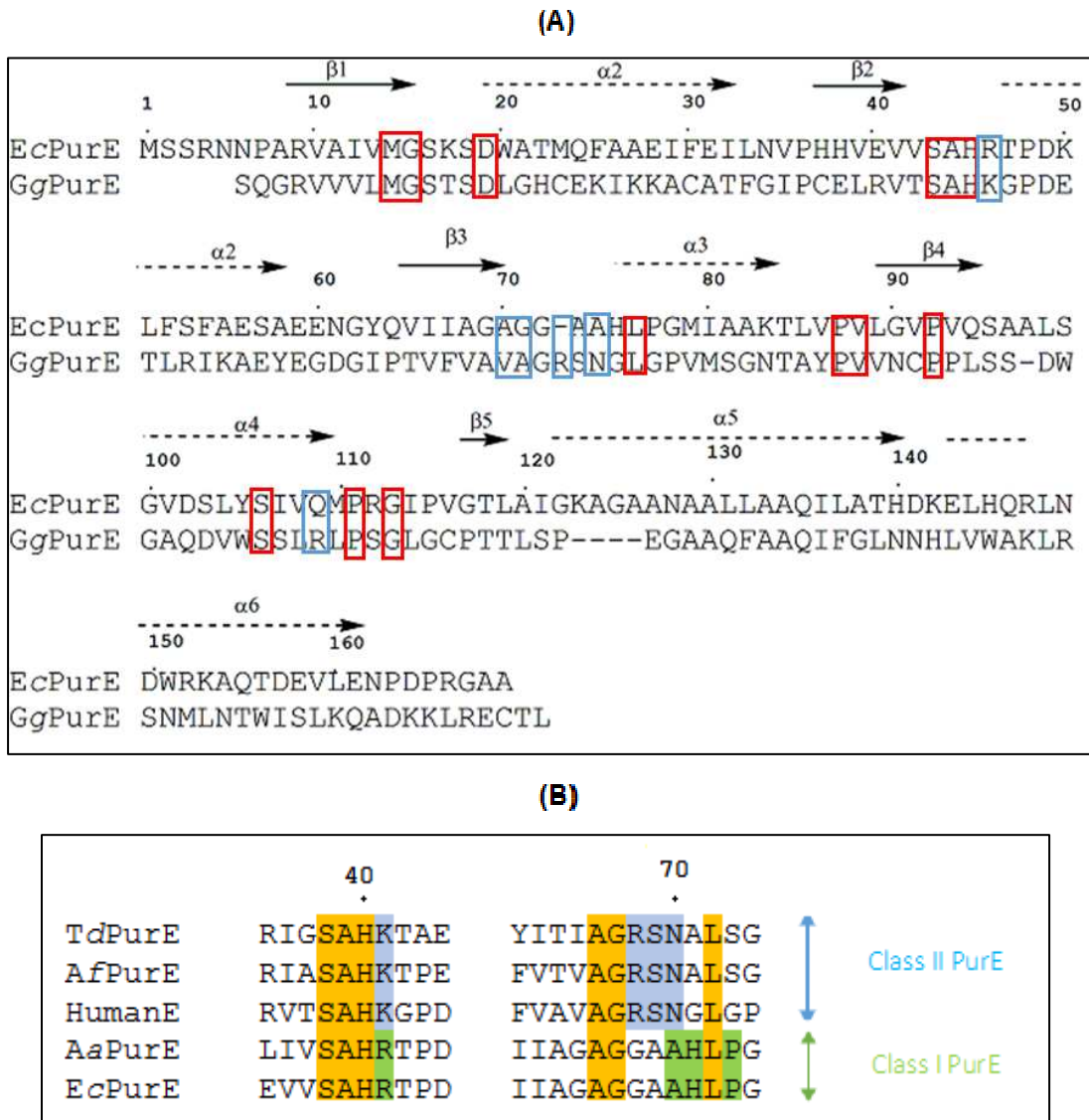


**Figure 3. Sequence alignments between Class I and Class II PurEs. (A)** Alignments between *E. coli* PurE and *G. gallus* PurE. Red cubes indicate universal conserved residues, and blue cubes indicates class specific residues. Sequence numbered after *E. coli* PurE. **(B)** Sequence alignments in 40S and 70S loop numbered after *Td* PurE. Orange represent the universal conserved residues, green is Class I specific conserved residues, and blue is Class II specific conserved residues. *Td* is *Treponema denticola*; *Af* is *Archaeoglobus, fulgidus*; *Aa* is *Acetobacter aceti*; *Ec* is *Escherichia coli*

Previous studies of Class I and Class II PurEs have shown how similar these two enzymes are to one another. The crystal structures (**Figure2**) show that they are both symmetrical octamers formed by similar 17KD subunits.<sup>14,15</sup> In humans, Class II PurEs are fused with SAICAR synthetase (PurC), while bacterial Class I PurEs are usually expressed alone. For yeast and fungi, Class I PurEs are usually fused with PurK. The sequence alignment of Class I and II from different species indicates that both have several conserved regions (**Figure 3A**). P-loop, which is between the  $\beta 1$  and  $\alpha 1$ , is responsible for phosphate group. 40s loop is located between  $\beta 2$  and  $\alpha 2$ , and 70s loop is located between  $\beta 3$  and  $\alpha 3$ .<sup>14,16</sup> Sequences alignments of Class I and II PurEs in the 40s and 70s loops indicates that S38, A39, H40, A66, G67, and L72 are highly conserved amino acid residues for all PurEs (**Figure3 B**). However, there are residues which are only conserved in each class. In the 40s and 70s loop, Class I PurEs' residues are conserved in R41, G68, A69, A70, H71, P73, while most Class II PurEs have K41, G68, S69, N70, G71, S73 at the same residues.<sup>11,15</sup> One of the special case of Class II PurEs is *Treponema denticola* (Td) PurE, which is the only known bacterial AIR carboxylase.<sup>16</sup>

The question of how these two similar enzymes catalyze different reactions is still unknown. The hypothesis is that the class specific conserved residues might be the key to determining the functional differences between these two classes of enzymes. However, few studies have been done on these residues and we don't know which residues are important for the specificity of

the reaction. To investigate this issue, we conducted site-direct mutagenesis to convert conserved amino residues (41, 68, 69, 70, 71, and 73) of wild type *Escherichia coli* into residues which mimic those found in Class II PurEs. Mutants were then investigated to determine, which, if any, mutation produced a change in the specificity of the enzyme reaction.

## 1.2. Results

The previous study of crystal structures of PurE shows that the active sites of PurEs are located in the P, 40s and 70s loops. Since the conserved residues on the P-loop are universally conserved, we did not alter these residues.<sup>15</sup> We focused on the class-specific conserved residues found in the 40s and 70s loops to investigate whether these residues affected the functional divergence between the two classes of PurEs.<sup>16</sup>

Arg41, Gly68, Ala69, Ala70, His71 and Pro73, (numbered by Td PurE, (**Figure 3B**), are Class I PurE conserved residues and we mutated each of these residues to that found in the human region.<sup>a</sup> This gave mutants R41K, G68R, A70N, H71G and P73S. Since *T.denticola* PurE is a bacterial Class II PurE we also mutated His 71 to alanine.

We investigated each of these mutants using developed assays, and compared them to the same kinetic studies of WT *E.coli* PurE. These studies were done to determine which amino acid(s) will decide the functional divergence between the two classes of PurEs.

### 1.2.1. Enzyme expression and purification

The cloning of PurE and plasmid purification was done by Aiko Hirata. The single mutants made are R41K, G68R, A70N, H71A, H71G and P73S. All plasmids were transformed into BL21/(DE3) competent cell for protein expression. All proteins were expressed and purified according to previously

---

<sup>a</sup> All the mutants cloning was done by Aiko Hirata from Dr. Fusao Hirata's group

developed procedures.<sup>17</sup> SDS-PAGE was utilized to check the protein purification of mutants. We obtained purified mutants R41K, G68R, A70N, H71A, and H71G. The P73S PurE, however, couldn't be expressed and was therefore not purified.

### **1.2.2. Protein folding of mutants**

#### **1.2.2.1. Limited proteolysis for WT and mutant PurEs**

In order to check whether the mutants are folding properly, limited proteolysis assays were performed. It is expected that a correctly folded enzyme will be relatively stable to the serine protease, subtilisin, whereas an unfolded protein would be degraded completely.<sup>18,19</sup> As showed in Figure 4, incubation of WT PurE with subtilisin for 1 hour leads to only a modest digestion as indicated by bands below the WT protein. This indicates that the protease only partly digests wild-type PurE. Analysis of mutants R41K, G68R, H71G and H71A with protease showed a pattern qualitatively similarity to the WT PurEs. However, A70N gave complete digestion indicating that this protein is partially unfolded or adopts an alternative conformation.

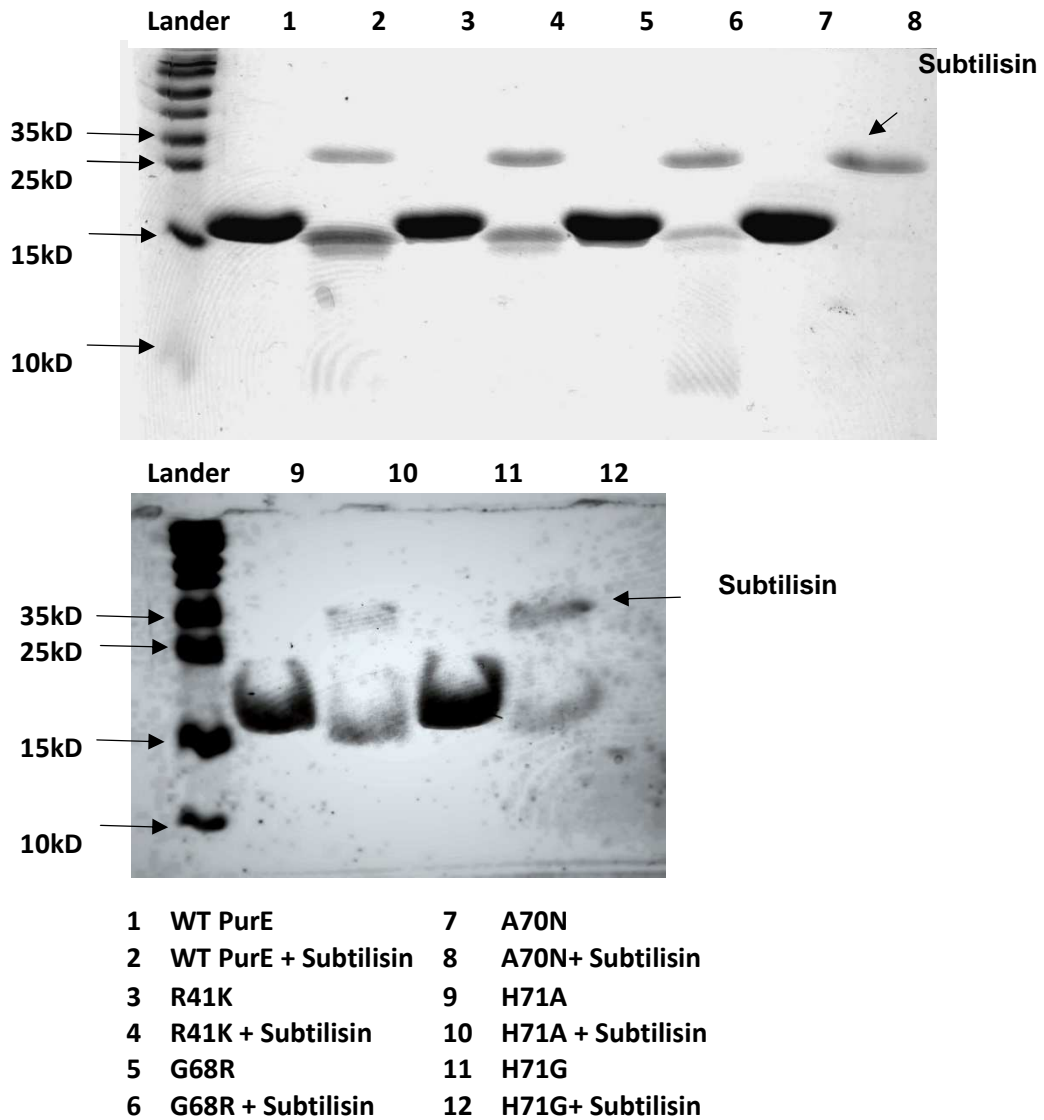


**Figure 4 SDS-PAGE (15%) of 18  $\mu$ g of wild-type or mutant (17kD) PurEs incubated with 18  $\mu$ g subtilisin (27kD) for 1 hour. The reaction were stopped by addition of PMSF. Gel were photographed and the contrast was adjusted to provide the image seen here**



### 1.2.2.2. Circular dichroism spectrum for folding of mutants

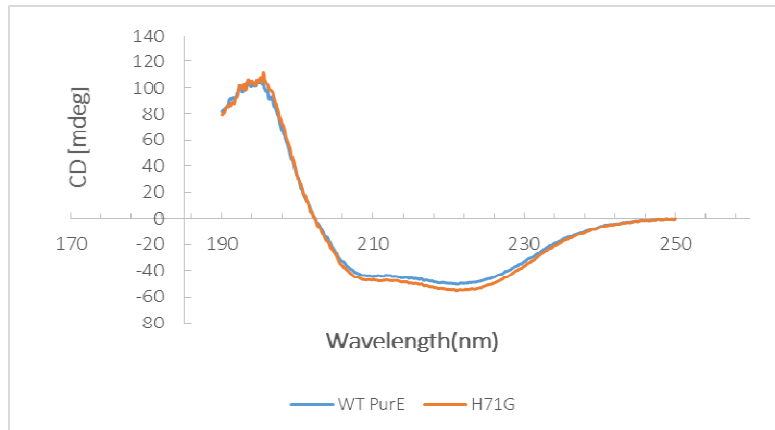


**Figure 5** Far-UV CD spectra of H71G and Wild Type PurE in 100 mM  $\text{Na}_3\text{PO}_4$  (pH, 7.4). The blue line represents 1.24 mg/mL of wild type PurE, while the red line is 1.15 mg/mL H71G.

Circular Dichroism (CD) can provide information on the structure of a protein. Usually, two UV regions are tested, the far-UV and near-UV. The absorption in the far-UV region (180nm-240nm) are mainly due to protein secondary structure ( $\alpha$ -helix,  $\beta$ -sheet, etc.), while the near-UV (250nm-290nm), where aromatic side chains can be detected, usually help to determine the tertiary protein structures.<sup>20,21</sup>

The far-UV CD spectra showed that no significant change of H71G secondary structure compared to WT PurE (**Figure 5**). Near-UV CD spectrum gave, no significant data for either WT PurE or H71G PurE. This result indicates that the H71G mutant is folded properly.

### 1.2.3. Steady-State kinetic analysis of the PurE mutants

The steady-state kinetic analysis for both WT and mutant PurEs was conducted using the CAIR decarboxylation assay.<sup>12</sup> Kinetic constants were determined by curve fitting a plot of velocity versus CAIR concentration to the Michaelis-Menten equation.<sup>22</sup>

**Table 3 Steady-State Kinetic Constants for Wild-type PurE and Mutants.  $V_{max}$  and  $K_m$  was determined by the CAIR decarboxylation assay system;  $k_{cat}$  was calculated using the molecular weight of the octamer.**

PurE Mutants	$V_{max}$ ( $\mu\text{mol}\cdot\text{min}^{-1}\cdot\text{mg}^{-1}$ )	$K_m$ ( $\mu\text{M}$ )	$k_{cat}$ ( $\text{min}^{-1}$ )	relative $k_{cat}/K_m$ (units/mg)	$k_{cat}/K_m$ $\text{min}^{-1}\cdot\text{M}^{-1}$
Wild type	54	38	7297	1	$1.9\times 10^8$
G68R	19	32	2538	0.35	$7.9\times 10^7$
A70N	0.6	473	75	0.01	$1.6\times 10^5$
H71G	6	16	800	0.11	$5.0\times 10^7$
H71A	8	15	1111	0.15	$7.4\times 10^7$
R41K	1.5	37	204	0.03	$5.5\times 10^6$

As shown in **Table 3**, the catalytic proficiency of all mutants, as expected, are decreased about 3-100 fold. Since A70N is not folded properly, it is not surprising to see its low binding affinity and catalytic proficiency. The  $K_m$  values are all within 2-fold of WT PurE suggesting that these mutants do not affect CAIR binding. The  $k_{cat}/K_m$  of WT and mutant PurEs are again similar. Overall, the kinetic studies indicate that these residues do not play a major role in either substrate binding or catalysis. Such a result may be expected given the fact that we made changes of conserved residues to amino acids that were conserved in the other class of PurE. A key question, though, is whether these mutants catalyze a different reaction from WT Class I PurE.

#### 1.2.4. Comparison of the CO<sub>2</sub> dependence of wild type PurE, human AIR carboxylases and mutant PurE

Previous studies have shown that CO<sub>2</sub> is the substrate only for AIR carboxylase. Class I PurEs are independent of the one-carbon substrate. However, N<sup>5</sup>-CAIR synthesis can occur non-enzymatically if enough CO<sub>2</sub> is provided. Therefore, one way to distinguish Class I and Class II PurEs (AIR carboxylase) is by examining their dependence on CO<sub>2</sub>.<sup>14</sup>

To determine this, reactions are examined at 10 °C, where the rate of equilibrium between CO<sub>2</sub> and HCO<sub>3</sub><sup>-</sup> is decreased. Thus, at early time points, the predominant one-carbon species is the one added. When CO<sub>2</sub> is added, AIR carboxylases rapidly converts AIR to CAIR.<sup>12</sup> Addition of bicarbonate gives no conversion. In contrast, when AIR is incubated with Class I PurE and CO<sub>2</sub>, no burst is observed.<sup>13</sup> In fact, often a decrease in absorbance is seen.<sup>23</sup> This decrease is due to the non-enzymatic turnover of AIR to N<sup>5</sup>-CAIR. At later times, CAIR production is seen as an increase in absorbance.

As shown in **Figure 6**, addition of CO<sub>2</sub> to WT PurE (blue line) generates a curve which shows a lag followed by an increase of CAIR production. Addition of CO<sub>2</sub> to human AIR carboxylase (yellow line) gave a burst in CAIR formation. These results were used as controls for mutants. Incubation with bicarbonate, results in no or modest CAIR formation for either WT PurE, AIR carboxylase or the mutants (**Figure 7**).

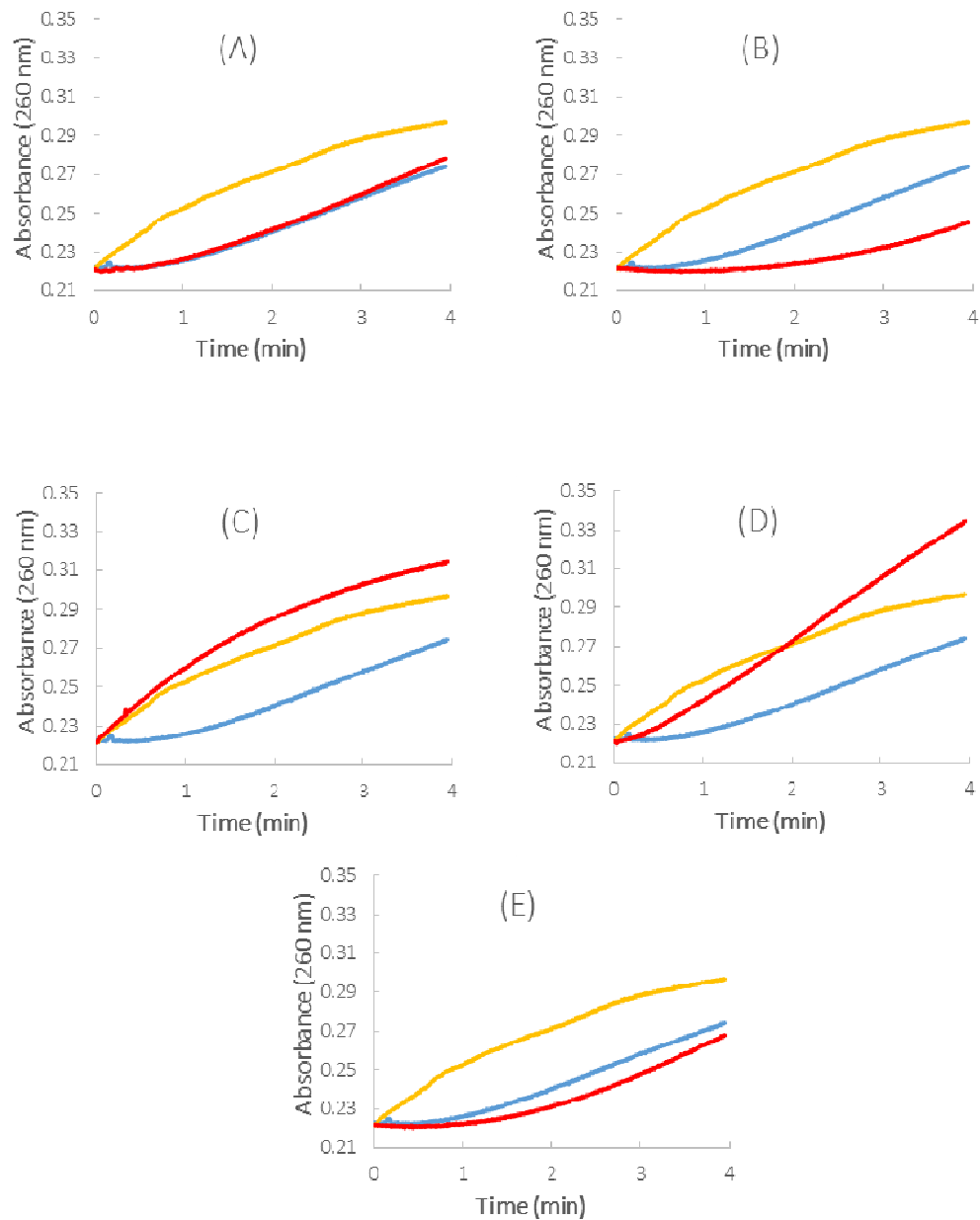


**Figure 6.** 150 μm AIR incubated with wild type or mutants PurE in the presence of 20 mM CO<sub>2</sub>. Yellow line is the absorbance of 600 ng human AIR carboxylase incubated with CO<sub>2</sub>, blue line is the 180ng *E.coli* PurE incubate with CO<sub>2</sub>. Red line shows each mutants with CO<sub>2</sub> 20 mM with same specific activity (0.01 μm·min<sup>-1</sup>). For comparison, the data for WT PurE and AIR carboxylase is shown with each mutant. (A) G68R 800 ng; (B) A70N 27 μg; (C) H71G 1.3 μg (D) H71A 1.2 μg (E) R41K 5.8 μg

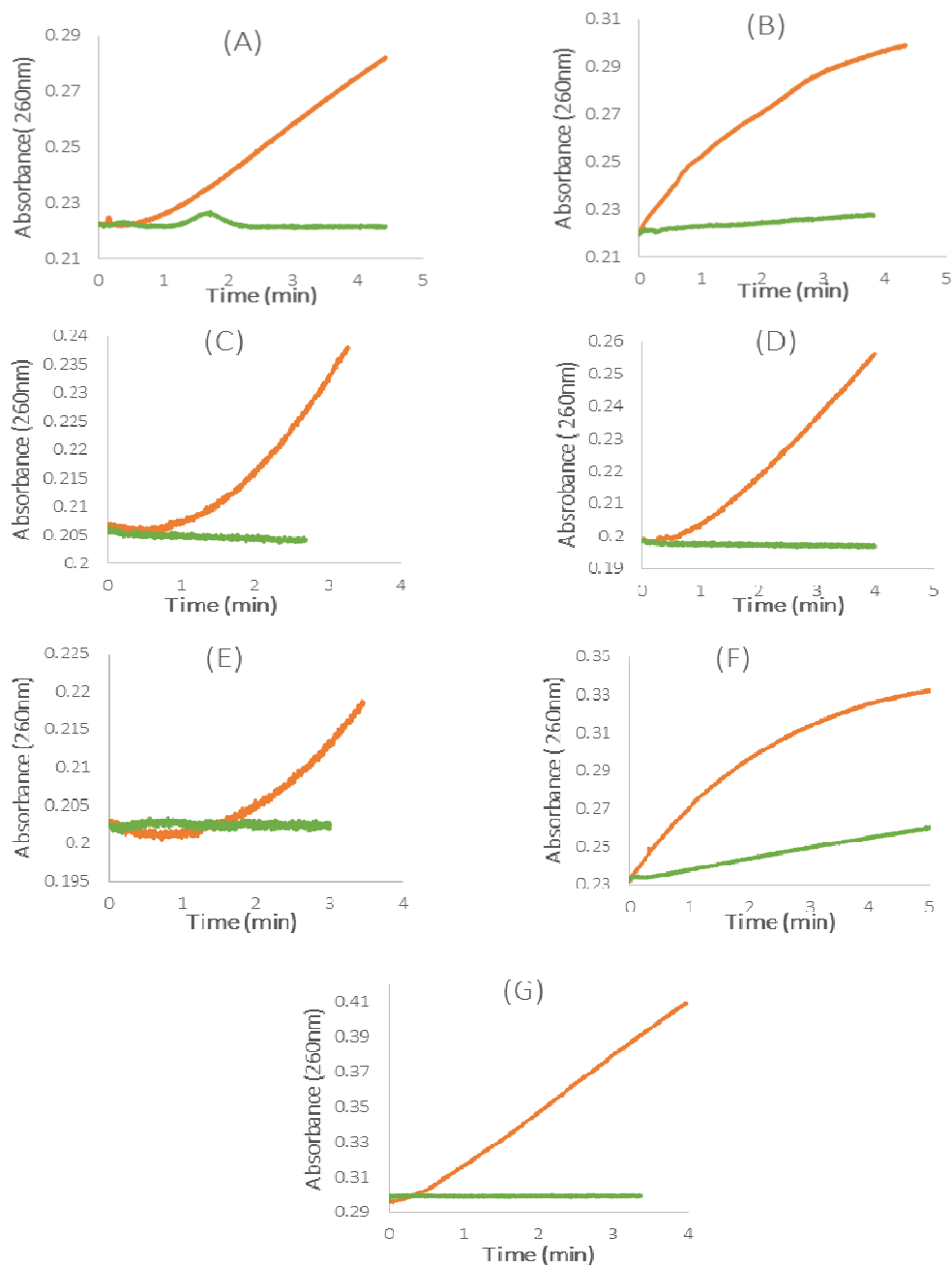


**Figure 7. Comparison of WT and mutant PurEs with  $\text{CO}_2$  or  $\text{HCO}_3^-$ . Orange lines represent enzymes incubated with 20mM  $\text{CO}_2$ , green lines are enzymes with 20 mM  $\text{HCO}_3^-$ . (A) Wild-type PurE 180ng (B) Human AIR carboxylase 600 ng ; (C) R41K 5.8  $\mu\text{g}$ ; (D) G68R 800 ng; (E) A70N 27  $\mu\text{g}$ ; (F) H71G 1.3  $\mu\text{g}$  ;(G) H71A 1.2  $\mu\text{g}$ .**

G68R, R41K and A70N all show obvious delays(**Figure 6**)when incubated with  $\text{CO}_2$ . This indicates that  $\text{CO}_2$  is not a substrate for these three mutants.

H71G shows a burst upon the addition of  $\text{CO}_2$  and a slow increase when  $\text{HCO}_3^-$  added. This is very similar to the curve generated with AIR carboxylase (**Figure 7 B&F**) with  $\text{CO}_2$ . In addition, it is interesting that the rate of CAIR production is greater than for human AIR carboxylase. In order to verify that  $\text{CO}_2$  was a substrate for H71G, carbonic anhydrase was introduced into the assay. Carbonic anhydrase rapidly establishes the equilibrium between  $\text{CO}_2$  and bicarbonate.<sup>24</sup> As showed in **Figure 8**, in the presence of carbonic anhydrase, the rate of CAIR production incubated with  $\text{CO}_2$  decreases due to rapid conversion of  $\text{CO}_2$  to bicarbonate. In contrast, incubation of H71G with bicarbonate and carbonic anhydrase leads to an increase in rate of CAIR production. This evidence shows that  $\text{CO}_2$ , but not  $\text{HCO}_3^-$ , is the substrate for H71G.

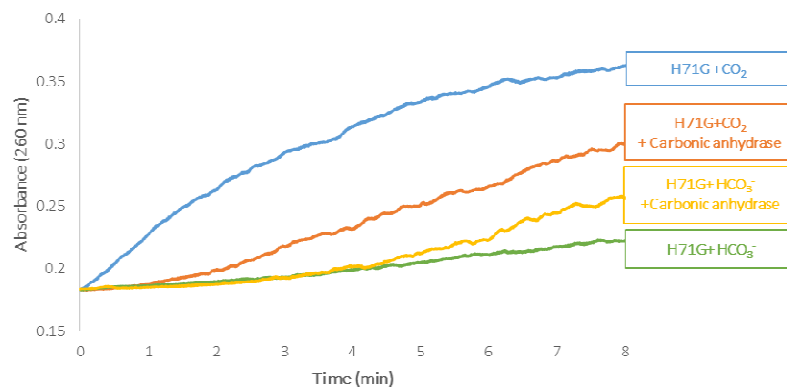


**Figure 8 Mutation H71G with one-carbonate substrates incubated with 1  $\mu\text{g}$  carbonic anhydrase.**

H71A is another interesting mutant. Incubation with  $\text{CO}_2$  does not generate a burst, however CAIR production is much more rapid than for WT PurE. Incubation with  $\text{HCO}_3^-$  curve indicates that  $\text{HCO}_3^-$  is not the substrate for H71A. Thus, H71A appears to be a hybrid between Class I and Class II PurEs. The analysis of the use of  $\text{CO}_2$  as a substrate revealed that H71G and perhaps H71A could utilize  $\text{CO}_2$ . This is a hallmark trait of AIR carboxylase and suggests that H71G may be an AIR carboxylase enzyme. However, these experiments do not indicate whether H71G has the ability to still utilize  $\text{N}^5$ -CAIR as a substrate.

#### **1.2.5. The PurC-coupled assay**

In order to determine whether AIR or  $\text{N}^5$ -CAIR is the substrates for H71A and H71G, we used a PurK/PurC coupled assay (Figure 9). This assay was done to produce  $\text{N}^5$ -CAIR in situ and to make CAIR production irreversible by converting it to SAICAR. SAICAR production is monitored at 282nm to indicate the production of CAIR.<sup>13</sup> In the absence of PurK (Figure 10 A), almost no SAICAR is produced from AIR by WT *E.coli* PurE. In addition, this demonstrates that the non-enzymatic synthesis of  $\text{N}^5$ -CAIR is not sufficient for turnover. This indicate that AIR, as expected, is not a substrate for WT PurE. In the contrast, addition of H71G or H71A gave an increase in SAICAR production, showing the AIR converted to CAIR in the absence of its conversion to  $\text{N}^5$ -CAIR by PurK.

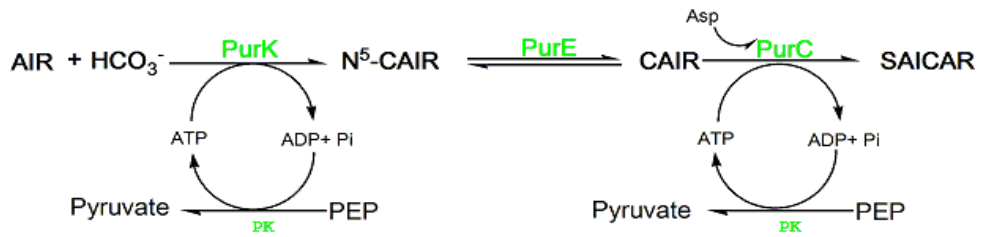


**Figure 10 PurC coupled assay**

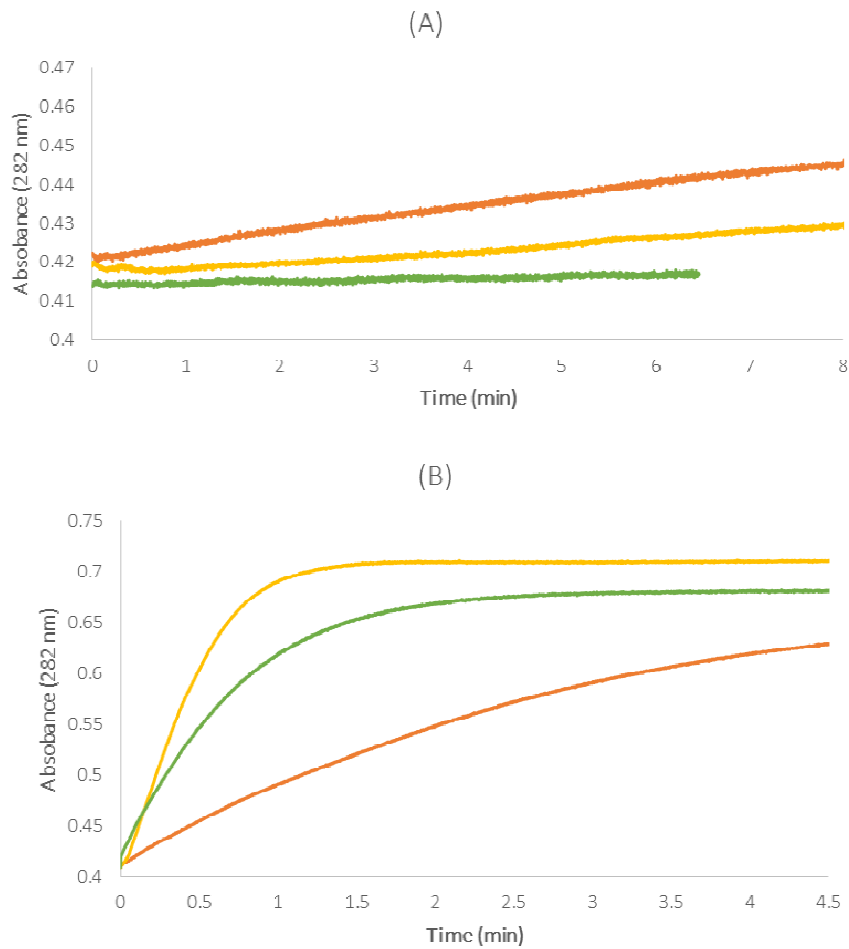


**Figure 10 PurC coupled assay to monitor N5-CAIR turnover. Green lines are 325 ng WT PurE; Yellow lines are 2 µg H71A; Red lines are 3 µg H71G. (A) Enzymes incubated without PurK; (B) enzymes incubated with 1.1 µg PurK.**



Addition of excess PurK leads to the rapid conversion of AIR in to N<sup>5</sup>-CAIR, and consequently, SAICAR is produced rapidly with WT PurE (**Figure 10B, green line**). This validates that N<sup>5</sup>-CAIR is the substrate of PurE. Interestingly, H71G also gave a burst of SAICAR production in the presence of PurK (**Figure 10B, red line**). The rate, however is lower than WT PurE. H71A shows a large burst of SAICAR production and appears it be faster than for WT PurE (**Figure 10B, yellow line**).

These results indicate that AIR is a substrate for both H71A and H71G. However, each protein also appears to utilize N<sup>5</sup>-CAIR as a substrate. Thus, H71A and H71G are both AIR carboxylase and N<sup>5</sup>-CAIR mutase enzymes. This data suggests that His71 plays a critical role in the reaction specificity of these enzymes.

### 1.3. Discussion

The purpose of the site-directed mutagenesis of N<sup>5</sup>-CAIR mutase is to find possible amino acid residues that might determine the functional divergence between Class I and Class II PurEs. Therefore, the residues chosen in this study are in the active sites of both Class I and II PurEs and, also, are specifically conserved in each type of PurE. We then mutated *E.coli* PurE conserved residues in the 40s and 70s loop to the corresponding conserved residues in human AIR carboxylase. We also mutated His71 to alanine because it is found in the only known bacterial AIR carboxylase, *Treponema denticola* PurE.<sup>16</sup> For these studies, we were able to express and purify, mutants R41K, G68R, A70N, H71G and H71A<sup>b</sup>.

We examined the steady-state kinetics using CAIR which is a substrate for both classes of PurE. All mutants, except for A70N, are active with  $k_{cat}$  values between 2 to 35 folded lower than WT *E.coli* PurE.  $K_m$  values are roughly the same as WT PurE. A70N was excluded as it is folded incorrectly and its catalytic ability and binding affinity was very low. The kinetic studies indicated that the enzymes were active, but the assay could not provide information on what product, AIR or N<sup>5</sup>-CAIR, is produced from CAIR. Thus, the study could not determine whether the mutants are N<sup>5</sup>-CAIR mutases or AIR carboxylase.

---

<sup>b</sup> All numbered after the *T. denticola* PurE sequences

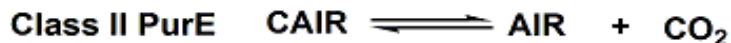
A key difference between N<sup>5</sup>-CAIR mutase versus AIR carboxylase is the fact that AIR carboxylase uses CO<sub>2</sub> as a substrate and N<sup>5</sup>-CAIR mutase does not. Therefore, we evaluate whether CO<sub>2</sub> was a substrate for the mutants. All mutants were studied at the same specific activity to ensure that any burst of CAIR production was due to CO<sub>2</sub> and not elevated enzymes level. The experiments were also run at 10 °C to slow the kinetics of the CO<sub>2</sub>/HCO<sub>3</sub><sup>-</sup> equilibrium. The results indicates that H71G and maybe H71A utilized CO<sub>2</sub> as a substrate. This suggests that these mutants are AIR carboxylase.

The next question is whether N<sup>5</sup>-CAIR is still a substrate. To answer that question, we utilized the PurC coupled assay investigating the forward reaction. In this assay, PurC is added, in the presence or absence of PurK, to monitor CAIR synthesis via SAICAR production. In the absence of PurK, H71G and H71A produced SAICAR from AIR and residual CO<sub>2</sub>. This confirms the AIR carboxylase activity. However, addition of PurK results in a large burst of SAICAR production indicating that N<sup>5</sup>-CAIR is also a substrate. This assay shows that H71G and H71A can utilize both AIR and N<sup>5</sup>-CAIR as substrates. This demonstrates that the H71G and H71A mutants are both N<sup>5</sup>-CAIR mutase and AIR carboxylase enzymes.

Based on these studies, His 71 seems to be very interesting residue and plays an important role in determine the functional divergence between human and bacteria PurEs.

### 1.3.1. Possible mechanism the conversion of N<sup>5</sup>-CAIR to CAIR.

#### Scheme 2 Simple mechanistic model for Class I and Class II PurEs



Currently, the most plausible mechanism for Class I PurEs is shown in **Scheme 2**. CAIR is first reversibly decarboxylated to the intermediate AIR·CO<sub>2</sub> complex which is then reversibly converted to N<sup>5</sup>-CAIR. Class II PurEs appears to only catalyze the first reversible conversion, CAIR to AIR·CO<sub>2</sub>.<sup>23,25</sup> Structure studies on the active site of PurEs show that the aminoimidazole ring of CAIR is in the hydrophobic pocket of Class I PurE formed by conserved residues located in the 40s and 70s loops.<sup>15</sup> The CO<sub>2</sub> generated from CAIR decarboxylation is believed to bind at the bottom of the active site. Therefore, mechanistic and structural studies indicate that Class I PurEs can trap CO<sub>2</sub> in the active site for the attacking AIR to produce N<sup>5</sup>-CAIR. Class II PurEs allow CO<sub>2</sub> to dissociate from AIR and, therefore, prevent the production of N<sup>5</sup>-CAIR.<sup>14</sup> However, Class II PurEs must also facilitate the binding of CO<sub>2</sub> for CAIR formation. How this occurs is unknown.

### 1.3.2. What role does His71 play in this mechanism?

Structure studies on *Acetobacter acetii* PurE (Class I PurE) indicates that His59 and His89 (TdPurE His40 and His71) are in contact with the His59 and His89 from their neighboring subunits to form a twofold histidine chain. This chain is isolated from solvent and it has been speculated that the possible

function of this chain is to transfer protons from one site.<sup>26</sup> Several studies have been done with these two histidine residues. His59 is a universally conserved residues in both Class I and Class II PurEs and is believed to be the general base needed for the reaction to form CAIR.<sup>14</sup> Site-direct mutagenesis studies on this residue indicates that it is essential as mutation to other amino acids abolishes activity.<sup>27</sup> On the other hand, our study on His71 agree with other's studies which show that site-direct mutagenesis of His71 decreases the enzyme activity but the enzyme is still functional.<sup>26,27</sup> However, examination on the reaction catalyzed by this mutant revealed that it has AIR carboxylase activity. Such a result has not been previously reported.

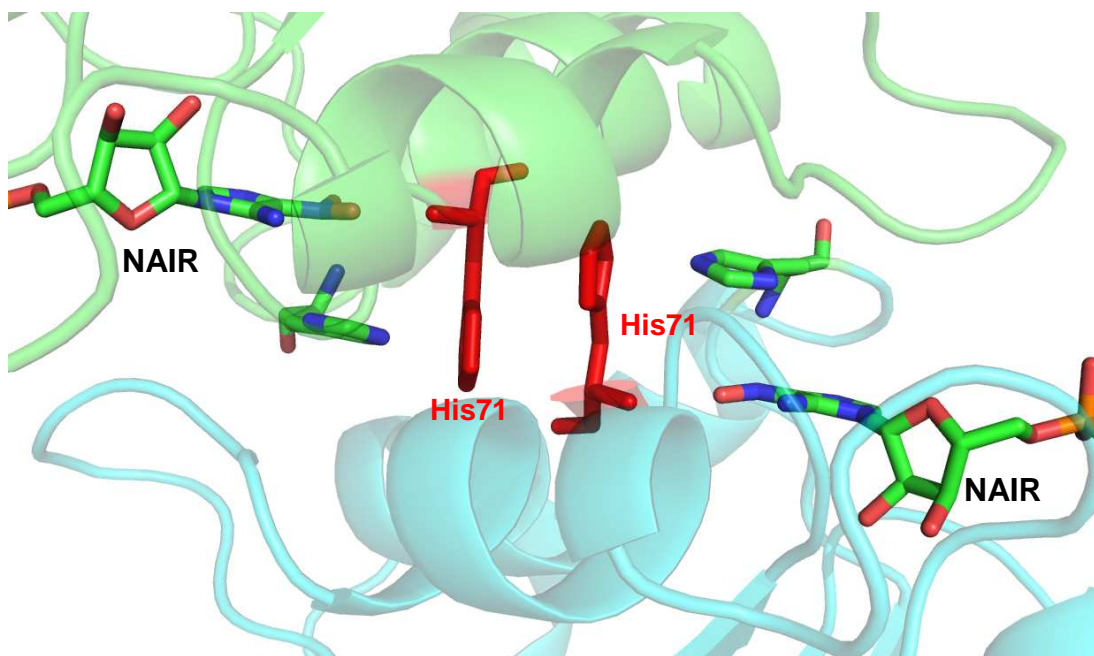
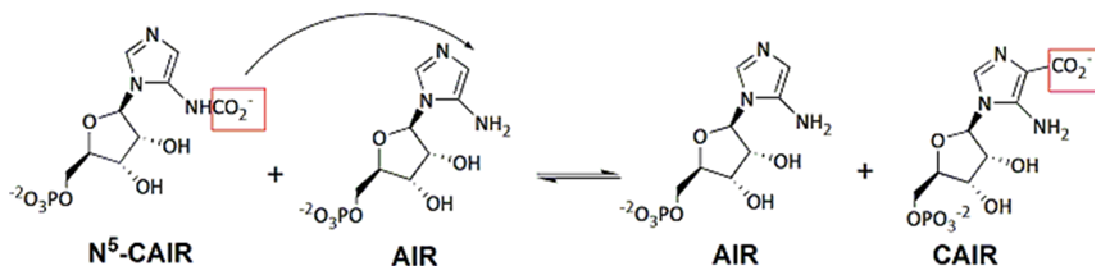


**Figure 11. Dimer structure of WT Class I PurE (2ATE). His 75 (same as TdPurE His 71) is shown in red. NAI is an analogue of CAIR and shown to indicate the substrate binding site in the active site position.**

Based on the previous mechanism and the crystal structures, we hypothesize that mutating the His71 residue leads to the opening of a channel between the two active sites from two monomers in the PurE octamer. The open channel between the two active sites may provide an avenue for CO<sub>2</sub> to dissociate from the AIR·CO<sub>2</sub> complex. Thus, H71G can partition between either CO<sub>2</sub> escape, leading to the generation of AIR or reaction with CO<sub>2</sub> to generate N<sup>5</sup>-CAIR. It is important to recognize, however, that the CO<sub>2</sub> must also bind to the H71G as the PurC assay in the absence of PurK, indicated turnover from AIR. How CO<sub>2</sub> binds and what is the driving force for this binding is unclear.

### 1.3.3. The open channel hypothesis for AIR carboxylase

**Scheme 3. Transfer model of CO<sub>2</sub> from N<sup>5</sup>-CAIR to AIR**



Early studies indicated that N<sup>5</sup>-CAIR was utilized as a carboxylase intermediate for transferring CO<sub>2</sub> and AIR to the PurE active site and the use of a carbamate was similar to the biotin-dependent carboxylase mechanisms.<sup>10,28,29</sup> One mechanism for N<sup>5</sup>-CAIR mutase was that N<sup>5</sup>-CAIR and AIR both bond to the site and CO<sub>2</sub> was transferred from N<sup>5</sup>-CAIR to AIR to generate AIR and CAIR (**Scheme 3**). However, structural studies indicate that the active site of Class I PurE does not have enough space for binding both N<sup>5</sup>-

CAIR and AIR. The opening channel, as hypothesized above, may provide a CO<sub>2</sub> tunnel between two isolated active sites. Thus, CO<sub>2</sub> dissociated from N<sup>5</sup>-CAIR in one active site may migrate through the channel to bind AIR in the connecting active site to produce CAIR. Such a mechanism model indicates that both N<sup>5</sup>-CAIR and AIR are substrates for AIR carboxylase. The CO<sub>2</sub>-dependence on the reaction could be explained by the rapid production of N<sup>5</sup>-CAIR which then delivers the CO<sub>2</sub> to the enzyme. N<sup>5</sup>-CAIR itself would not be turned over until enough AIR was produced to occupy the other active site.

#### **1.4. Future Studies**

According to the results and discussion above, we make a hypothesis that His 71 might be the critical conserved residue to determine the functional difference and removal of histidine may open a channel between two active sites for CO<sub>2</sub> transferring. Therefore much more studies can be applied to prove that.

Some Crystal structure studies should be done to prove whether the open channel exists and whether they can let CO<sub>2</sub> go through. Also, there are some mutants that have not been made properly, which might also be important to determine or assist His 71 to determine the functional differences.

Further studies on this mechanism will need to be done to validate this proposed mechanism.

## Chapter 2.

### Developing a High-Throughput Screening Assay for the Discovery of N<sup>5</sup>-Carboxyaminoimidazole Ribonucleotide Mutase Inhibitors

#### 2.1. Introduction

##### 2.1.1. Drug Resistance and new antibiotics

Since the 1970s, only two new classes of antibiotics (Linezolid, and Daptomycin) have been introduced to the market.<sup>30</sup> However, infections due to resistant organisms have become much worse.<sup>31,32</sup> Therefore, there is an urgent need for new targets of antibiotics.

##### 2.1.2. PurEs as a new target for antibiotic drug discovery

The *de novo* purine biosynthetic pathway could be a potential target for the development of new antibiotics because the pathway is different between humans and bacteria.<sup>5</sup> As mentioned in the first part of the thesis, Class II PurEs, found in humans, directly catalyze the conversion of AIR to CAIR, while Class I PurE, found in bacteria, turns N<sup>5</sup>-CAIR to CAIR.<sup>6</sup> While Class I and Class II PurEs are similar, they each catalyze their own reaction and selective inhibition by NAIR suggests that small molecules can be found which can selectively inhibit one class over other.<sup>33</sup> Therefore, PurEs could be a new antimicrobial drug target.

##### 2.1.3. High-throughput screening

High-throughput screening (HTS) is utilized in drug discover, because it can screen thousands of compounds in a short period and can provide



potential “hits” for follow-up studies.<sup>34</sup> Critical to the success of a HTS is a robust and rapid assay which is capable of detecting enzyme catalysis in a small volume with great sensitivity. A HTS assay must be rapid, sensitive and free from interference by other parts of the assay. A number of techniques have been used for HTS assay mostly fluorescence, absorbance, FACS and even imaging.<sup>35</sup>

#### **2.1.4. Limitation of CAIR decarboxylase assay**

Since no small molecule non-nucleotide inhibitors are known for N<sup>5</sup>-CAIR mutase, the Firestine lab conducted a HTS based on the CAIR decarboxylase assay. While the assay worked, only one selective inhibitor was found and the assay suffered from false negatives. The possible reason for the unsuccessful HTS for N<sup>5</sup>-CAIR mutase inhibitors is the limitations of the CAIR decarboxylase assay.<sup>12</sup> This assay is based on observing an absorbance change of CAIR at 260nm. Unfortunately, many organic small molecules also absorb in this region. To circumvent this problem, the absorbance of the compound was subtracted from each well. However, for highly absorbent compounds, this often lead to concerns over measuring the small change in CAIR absorbance due to catalysis. The potential inhibitors might be missed during the HTS. It is clear that a better HTS assay is needed for screening for inhibitors of N<sup>5</sup>-CAIR mutase. In this chapter, we will discuss the assessment of several potential assays for HTS of N<sup>5</sup>-CAIR mutase.<sup>36</sup>

## 2.2. Results and discussion

### 2.2.1. AIR carboxylation assay

Another classic assay for the study of PurE activity besides CAIR decarboxylation is the coupled N<sup>5</sup>-CAIR mutase assay which measures the conversion of N<sup>5</sup>-CAIR to CAIR by the production of SAICAR. This assay starts with AIR which is rapidly converted to N<sup>5</sup>-CAIR by PurK. Conversion of N<sup>5</sup>-CAIR to CAIR is monitored by SAICAR synthetase at 282 nm or at 340 nm for ATP assumption.<sup>10,13</sup> However, this assay not appropriate for HTS as several enzymes (PurK, PurC, PK, LDH and NADH) are involved and, therefore, it is hard to tell if the hits generated from HTS inhibit PurE the coupling enzymes. Thus, extensive deconvolution would be needed limiting its usefulness for HTS.

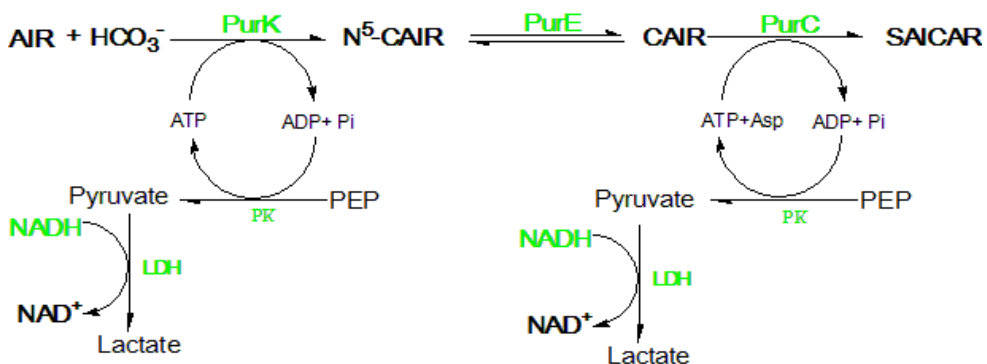
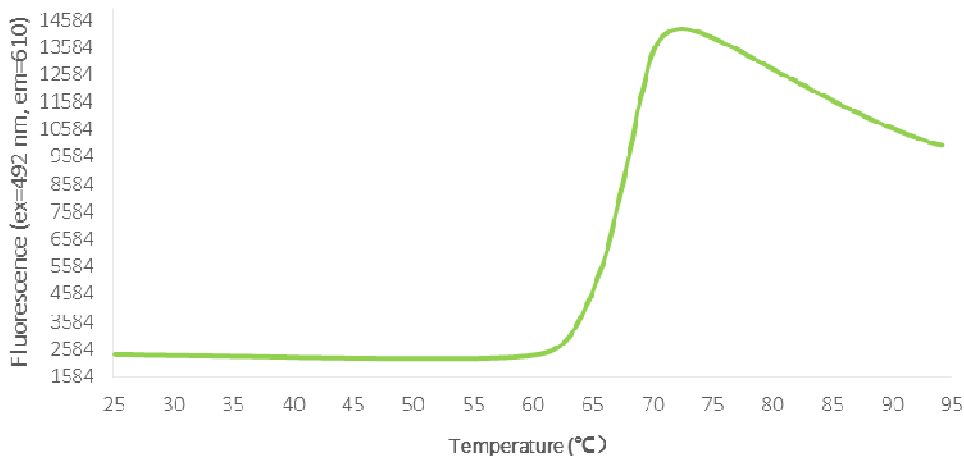


Figure 12 Procedure of PurC coupled assay.

### 2.2.2. Thermoflour®



**Figure 13 Fluorescence intensity versus temperature for unfolding PurEs in the presence of SYPRO orange (ex=492 nm, em=610 nm).**

The thermoflour® assay is based on measuring the changes in the protein melting temperature ( $T_m$ ) upon the binding of a ligand (inhibitor).<sup>37</sup> Previous studies have shown that binding of small molecules can alter a protein's melting temperature, by either stabilizing or destabilizing the folding of the protein.<sup>38</sup> Therefore, compounds which bind to Class I PurEs could theoretically be screened by this method.

For PurE, we followed the standard assay determined by Nisesn, et al.<sup>39</sup> SYPRO orange (ex=492 nm, em=610 nm) is a fluorescent protein dye whose fluorescence increases when a protein unfolds. We utilized a real-time (RT)-PCR instrument to gradually increase the temperature from 25 to 95°C, while monitoring the fluorescence. The  $T_m$  was determined from the melting curve by calculating the maximum of the first derivative.

The melting curve of *E. coli* PurE is showed on **Figure 13**. PurE is stable until approximately 60 °C at which point the fluorescence intensity increases rapidly due to the unfolding of PurE. The signal decrease from 75 °C to 95 °C is due to protein precipitation or aggregation. The calculated  $T_m$  of PurE is  $68.12 \pm 0.03$  °C, as determined by 8 replicate experiments.

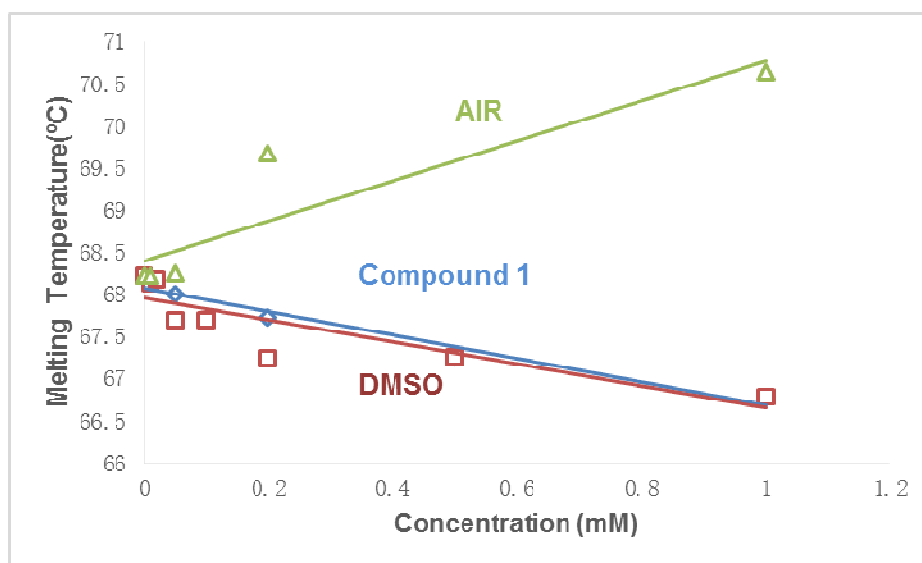


**Figure 14** The melting temperature versus the concentration of compounds. 75 µg/ml PurEs incubated with different concentration (0.01 –1 mM) of compounds. Green line is AIR; Blue compound 1 ( $IC_{50}=150$  µM); Red line is DMSO.

We next investigated the affect on the  $T_m$  as a function of inhibitor concentration. **Figure 14** shows the  $T_m$  versus compound concentration. AIR was used as a positive control, because previous studies have shown that it binds to PurE.<sup>14</sup> As expected, the fluorescence intensity increase as the concentration of AIR increased. Compound 1 {1-(4-ethoxyphenyl)-3-[(3-

pyridinylmethyl) amino]-2,5-pyrrolidinedione) studied as these were identified as binders in a fragment screening study for PurE inhibitors.<sup>40</sup> Preliminary experiments indicated that DMSO could affect the  $T_m$ , and the two compounds used in this experiment were dissolved in 100% DMSO. Therefore, we also measured the change in  $T_m$  at DMSO concentrations equivalent to what would be found for these two compounds. As shown in **Figure 14**, compound 1 and DMSO show an identical change. This indicates that both of the compounds have no significant affect on the PurE  $T_m$  change.

Why did we fail to measure a change in  $T_m$  for compounds which have been shown to bind to PurE? One possible reason is that the binding between PurE and these two compounds is not tight enough. Another possibility is that the  $T_m$  of PurE is fairly high, thus changes in the stability of the protein are small and so difficult to measure. Alternately, at high temperature, binding of the compound to the enzyme is poor due to the deformation of the binding site. Ultimately, despite much effort, we were unable to find a condition that allowed us to detect binding of various compounds by alternation in  $T_m$ . Therefore we abandoned this assay.

### 2.2.3. Metal stopping assay

#### 2.2.3.1. Assay design and hypothesis

Previous studies indicated that metal cations can chelate to CAIR so tightly that it stops PurE catalysis.<sup>41</sup> The tight binding of metals (such as Ni<sup>+</sup> and Zn<sup>2+</sup>) to CAIR suggested that this property may be useful to determine the concentration of CAIR, which in turn, could lead to a suitable assay for PurE.

Two questions need to be answered before such an assay can be developed: which metal to use and how to detect the CAIR:metal concentration. Previous studies indicated that Ni<sup>+</sup> and Zn<sup>2+</sup> tightly bind to CAIR and, therefore stop the reaction. Zn<sup>2+</sup> was chosen for our experiments as the previous studies showed that a CAIR:Ni<sup>+</sup> complex had poor kinetic stability.<sup>41</sup> To measure the concentration of CAIR-Zn<sup>2+</sup>, we utilized the Zn fluorescent dye, TSQ. When TSQ is incubated with Zn<sup>2+</sup>, a 1:2 complex is formed which is fluorescent (ex=360nm, em=490nm).<sup>42,43</sup> In the presence of a high CAIR concentration, zinc would bind to CAIR instead of TSQ and the fluorescence would decrease. Such a competition assay between TSQ, CAIR and Zn<sup>2+</sup> could provide a new assay for PurE. As CAIR decreases, due to PurE activity, more Zn<sup>2+</sup> would be available to bind to TSQ and the fluorescent signal will increase. Using this method, we can calculate how much CAIR is converted by the enzyme, and, therefore, deduce the kinetic data for the enzyme. Ultimately, this assay may be applicable for HTS.

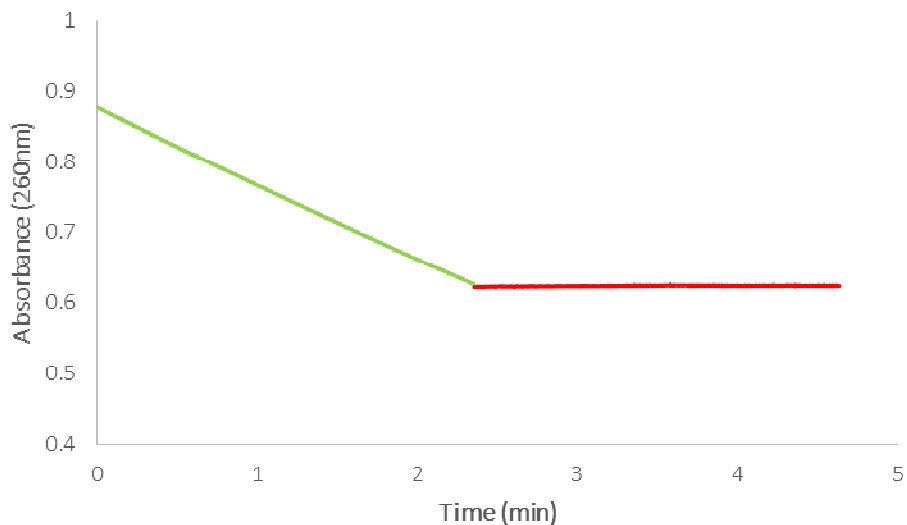


**Figure 15.  $Zn^{2+}$  stops PurE from converting CAIR to AIR. Green line is 60ng PurE incubated with 130  $\mu M$  CAIR at room temperature; red Line is when 250  $\mu M$   $ZnSO_4$  added.**

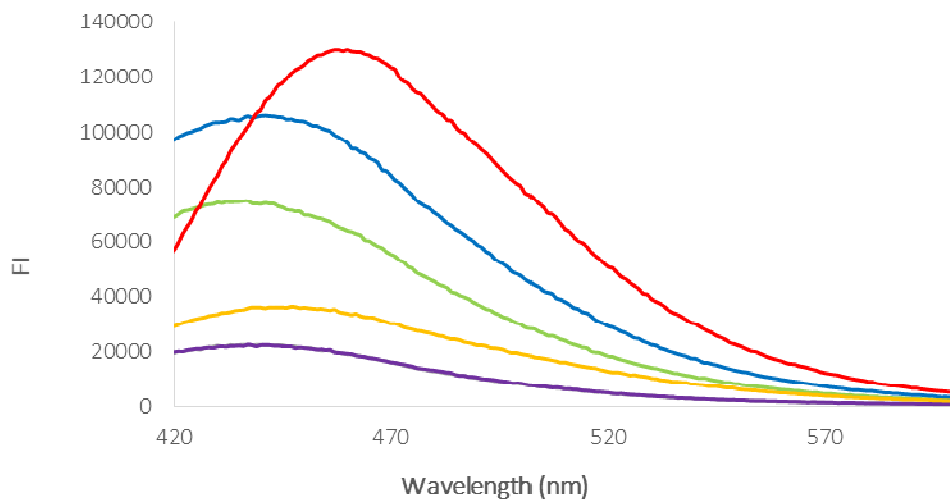


**Figure 16. Fluorescent signal scan (ex=360 nm) for Zinc, AIR and CAIR. Grey line is the buffer (50mM Tris-HCl, pH7), Purple line is 250  $\mu M$   $ZnSO_4$  in buffer; orange line is 250  $\mu M$  CAIR in buffer; Red Line is 250  $\mu M$   $ZnSO_4$  with 250  $\mu M$  CAIR in buffer; green line is 250  $\mu M$  AIR; and blue line is 250  $\mu M$  AIR with 250  $\mu M$   $ZnSO_4$ .**

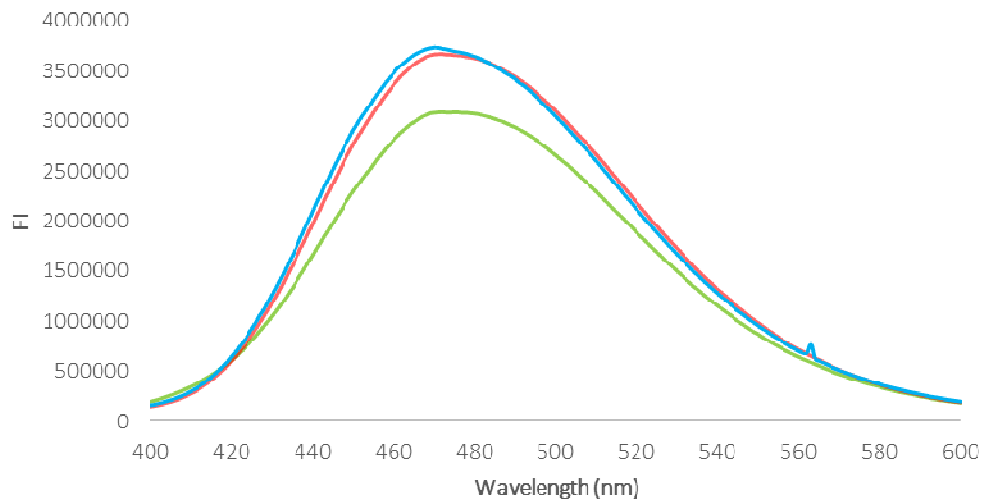


**Figure 17. Wavelength versus fluorescence (ex=360 nm). Green line is 100  $\mu\text{M}$   $\text{ZnSO}_4$  incubated with 50  $\mu\text{M}$  TSQ; Red line is when 50  $\mu\text{M}$  CAIR was added into solution; Blue line is 550  $\mu\text{M}$  CAIR was added.**

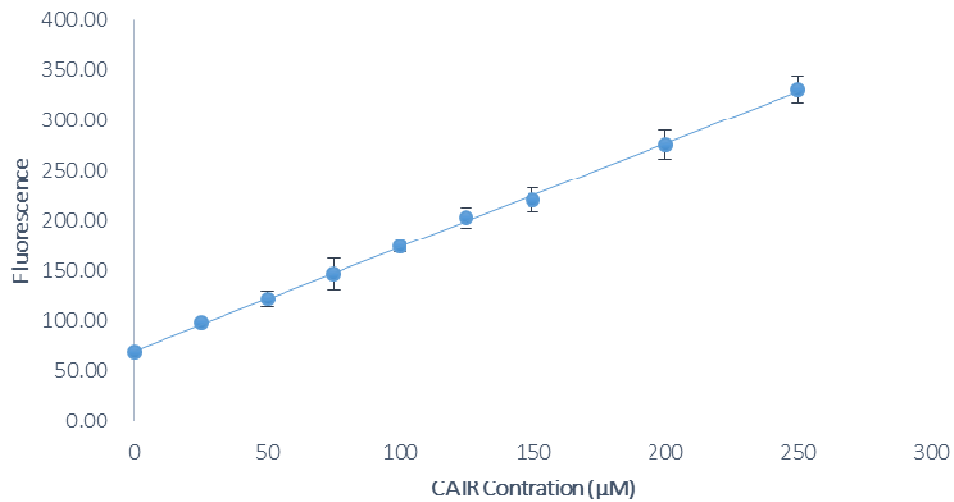


**Figure 18. CAIR concentration versus Fluorescence (ex=360 nm, em=485 nm). CAIR from 0 to 250  $\mu\text{M}$  incubated with 250  $\mu\text{M}$   $\text{ZnSO}_4$  in 96 wells plate. Each concentration of CAIR has 8 duplicates.**



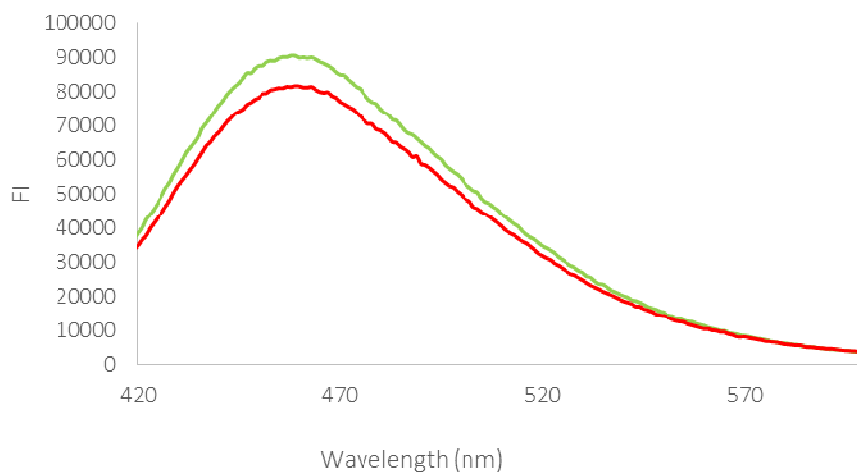


**Figure 19** Fluorescent signal scan (ex=360nm) with PurEs. Green line represent that 250  $\mu\text{M}$  CAIR incubated with 250  $\mu\text{M}$   $\text{ZnSO}_4$ , Red line is when 250  $\mu\text{M}$  CAIR incubated with 3  $\mu\text{g}$  *E.coli* PurE for 5 mins, 250  $\mu\text{M}$   $\text{ZnSO}_4$  was added to the mixture.

### 2.2.3.2. Experiments and results

Previous studies showed that 250  $\mu\text{M}$   $\text{ZnSO}_4$  totally stops *E.coli* PurE from converting CAIR to  $\text{N}^5$ -CAIR.<sup>41</sup> As shown in **Figure 15**, once  $\text{Zn}^{2+}$  is added, there is an immediate end to the PurE catalyzed conversion of CAIR to  $\text{N}^5$ -CAIR. Therefore, we utilized this condition.

Incubation of TSQ with  $\text{Zn}^{2+}$  gave the expected fluorescent signal. However, addition of CAIR failed to decrease the signal. Therefore, we checked all compounds used in this assay and interestingly, found that  $\text{Zn}^{2+}$  plus CAIR generated a strong fluorescent signal at 460nm (**Figure 16**). This signal is close to  $\text{Zn}^{2+}$ :TSQ complex fluorescent peak. Thus, we found that the  $\text{Zn}^{2+}$ :CAIR complex interfered with the monitoring of  $\text{Zn}^{2+}$ :TSQ complex formation.

Based on these results, we redesigned the assay, using the  $\text{Zn}^{2+}$ :CAIR fluorescent signal to calculate the CAIR concentration. As shown in **Figure 16** and **Figure 18**, as the concentration of CAIR increases the fluorescence increases linearly. This provides an easy method to calculate CAIR concentration. In order for this PurE assay to work, AIR must not form a strong complex with  $\text{Zn}^{2+}$  nor must it generate a strong fluorescent signal. As showed in **Figure 16**, incubation AIR with  $\text{Zn}^{2+}$  yielded a fluorescent signal, but one with an intensity much lower than CAIR. In addition, the emission peaks are different between these two complexes; the peak of AIR complex is about 439 nm while the CAIR complex peak shifts to 459 nm.

Despite this preliminary results, experiments with PurE showed that the assay is not sensitive. As shown in **Figure 19**, the fluorescent signal change can only be observed when a large amount of PurE is added. The amount of PurE needed (3  $\mu\text{g}$ ) is about 60 times that used in the decarboxylation assay. This would require a large amount of enzyme for HTS. In addition, the small change in signal could make the assay difficult to use in a screening system where only a modest inhibition is frequently observed. Since the assay is not sensitive, we decided not to continue to work on this method.

## Chapter 3

### Materials and Methods

#### 3.1 Materials

All chemical compounds come from Fisher, Sigma-Aldrich, or Thermo Scientific. E.coli PurE mutants were prepared in pET-21 with a C-terminal his-tag and contained additional sequences CTG GAG CAC CAC CAC CAC CAC CAC. These plasmids were cloned and amplified by Aiko Hirata. Sequences were verified by the DNA Sequencing Lab at Wayne State University. BL21 (DE3) was obtained from New England Biolab Inc.. E.coli PurC was the kind gift of Dr. T. Joesph Kappock (Purdue University, West Lafayette). Wild-type E. coli PurK was expression and purified by Jordan Rantucci.

All UV assays were conducted on a Cary 100 UV-vis spectrophotometer equipped with a temperature controller. Fluorescence was done using the Fluoro MAX®-3 with FluorEssence™ software. Circular Dichroism (CD) was conducted using Jasco J-1500 high performance CD spectrometer and access to this instrument was kindly provided by Dr. Timothy Stemmler. Thermal shift assays were conducted using the Mx3005P qPCR System and access to this instrument was kindly provided by Dr. Olivia Merkel.

#### 3.2 Expression and purification of WT and mutated PurEs

E.coli BL21/(DE3) was transformed with plasmids containing mutants or wild-type PurEs cloned into pET-21. A single colony was incubated overnight at 37 °C in 5 ml LB medium with 50 mg/L ampicillin and the overnight culture was

diluted (1:100) into 500 mL LB medium with 50 mg/L ampicillin and incubated until an  $OD_{600}$  of 0.5 was obtained. Protein expression was induced by the addition of 0.1 M IPTG and incubated for an additional 4 hours. Cells were centrifuged (20,000 rpm) and stored at -20 °C until use.

For purification, bacterial cells were lysed by addition of B-PER reagent (4 mL per gram of pellet, Pierce Biotechnologies) and incubated for 10 min. The resulting suspension was centrifuged at 20,000 rpm for 60 min (Beckman ultra-high-speed centrifuge, rotor JA-20) to remove cell debris. The clear supernatant was treated with streptomycin (5 mg/mL) and incubated for 2 hours before precipitated nucleic acids were removed by centrifugation at 20,000 rpm for 60 min. The supernatant was loaded, at 4 °C, onto a column (10 mL) containing Cobalt RAPID RUN™ Agarose Beads (Gold Biotechnology) which had previously been pre-conditioned with buffer A (10mM sodium phosphate, 300 mM sodium chloride, and 10 mM imidazole, pH 7.4). The column was successively washed, at 4°C, with Buffers A-D (Buffer A containing either 50 mM (B), 150mM (C), or 400 mM (D) imidazole). Fractions were collected and the PurE proteins eluted with buffer D. The purity of the protein was checked with 15% denatured SDS-PAGE. Purified PurE was dialyzed against 10 mM Tris-HCl, 200 mM NaCl, pH 8 and concentrated to at least 1 mg/mL using an Amicon® centrifugal concentrator. The protein was stored in -80 °C. Protein concentrations were determined using the Coomassie

(Bradford) Protein Assay Kit following the manufactures instructions (Thermo Scientific).<sup>36</sup>

### **3.3 Limited Proteolysis**

Limited proteolysis was conducted according to previous methods. (18) Briefly, wild type or mutant PurEs (18 µg) were added to 30 µL of buffer (50 mM Tris-HCl, pH 8.0) and 0.18 µg of subtilisin (from *Bacillus licheniformis*) was added. The reaction was incubated on ice for 1 hour at which time it was quenched by the addition of 1 mM PMSF. Products of the proteolysis were examined using a 15% denatured SDS-PAGE stained with Commassie Blue.

### **3.4 Circular Dichroism.**

Wild-type or mutant PurE was dissolved in buffer (NaPO<sub>4</sub> 100mM, pH 7.4) to a final concentration of 1 mg/ml. The protein sample (70-100 µL) was loaded in a 0.2 mm path length cuvette and the CD spectrum was obtained at room temperature for far UV (190-250nm) and near UV (260-320nm).<sup>44</sup>

### **3.5 Steady-state kinetic**

The assay contained 100 mM Tris-HCl (pH8), 6.25-150 µM CAIR and varied amounts of WT (48ng) or mutant PurEs (0.2-0.6 µg) in final volume of 1mL in a 1cm path length cuvette. (12) The consumption of CAIR was monitored at 260nm at room temperature. A plot of initial velocity versus substrate concentration was generated and the data was fitted to the Michaelis Menten equation (1) and kinetic parameters were calculated by Kaleidagraph (Synergy).<sup>22</sup>

$$v_0 = \frac{V_{max}[S]}{K_m + [S]} \quad (1)$$

### 3.6 CO<sub>2</sub>-dependence assay

To a stopper-fitted cuvette containing 100 mM Tris-HCl, pH 8, 3U of WT or mutant PurEs was added along with 125 μM AIR. The reaction was incubated at 10 °C for a min. In some experiment, 1μg/mL carbonic anhydrase was also added. Reaction was initiated by addition of 20 mM CO<sub>2</sub> or NaHCO<sub>3</sub>. CO<sub>2</sub> solutions were prepared by continuous bubbling CO<sub>2</sub> into 100mL distilled de-ionized H<sub>2</sub>O at 4°C and the concentration was estimated by the solubility constant of CO<sub>2</sub> (0.2871g/100g of water).<sup>13</sup>

### 3.7 PurC coupled assay.

A cuvette with a 1mL final volume containing 100 mM HEPES, pH 7.5 buffer, 20 mM KCl, 6 mM MgCl<sub>2</sub>, 2 mM PEP, 100 μM ATP, 10mM aspartic acid, 4 U of pyruvate kinase, 17 U lactate dehydrogenase and 100 μM NADH was incubated at 37 °C for 5 minutes. To this, *E. coli* PurC (13.5 μg) was added along with PurK (0 or 11.5 μg) and WT or mutant PurE (6U). The reaction was initiated by adding 60 μM AIR and SAICAR synthesis was monitored at 282 nm.<sup>9,10,45</sup>

### 3.8 Thermoflour®

In a 0.2 mL PCR tube, 10 mM HEPES (pH7.5) buffer was added along with 150 mM NaCl, 5X SYPRO Orange, and 75 μg/ml of *E. coli* PurE, (0-1mM) AIR or, 1-(4-ethoxyphenyl)-3-[(3-pyridinylmethyl)amino]-2,5-pyrrolidinedione

(ChemBridge Corporation). The final volume was 30  $\mu$ L, Thermal melting was done using a RT-PCR instrument from 25-95  $^{\circ}$ C while monitoring fluorescence of SYPRO orange (ex=492 nm, em=610 nm). The melting temperature was calculated from the maximum of first derivate curve.<sup>39</sup> For studies of ligand induced changed in the  $T_m$ , the same experiment was repeated in the presence of various concentrations of ligand.

### **3.9 Metal stopping assay.**

In a final volume of 1mL containing 50 mM Tris-HCl (pH 7) buffer, 250  $\mu$ M CAIR or AIR was added along with E.coli PurE (0-3  $\mu$ g) and the reaction was incubated at room temperature for 10 minutes. The reaction was quenched by the addition of 250  $\mu$ M ZnSO<sub>4</sub> and fluorescence was determined from 400-600 nm while being excited at 360nm. The same concentration and method was applied to a 96-well microplate using a 100  $\mu$ L per well final volume. Fluorescence data was collected using the Multi-Mode Microplate Reader (Synergy) with the excitation filter set at 360 nm and the emission filter set at 485 nm.<sup>41</sup>

## REFERENCE

1. Nyhan, William L. "Disorders of Purine and Pyrimidine Metabolism." *Molecular Genetics and Metabolism* 86, (2005): 25–33.
2. S. C. Hartman, J. M. Buchanan. "The Biosynthesis of the Purines." *Ergebnisse der Physiologie* (1959): 50-75.
3. Donald Voet, Judith G. Voet. *Biochemistry Fouth Edition*: JONH WILEY & SONS, INC, 2011.
4. Murray, Andrew W. "The Biological Significance of Purine Salvage." *Annu. Rev. Biochem*, (1971): 773-825.
5. Y. Zhang, M. Morar and S. E. Ealick. "Structure Biology of the Purine Biosynthetic Pathway." *Cellular and Moelcular Life Science*, (2008): 3599-3724.
6. Wakako Watanabe, Gen-Ichi Sampei, Atsu Aiba, Kiyoshi Mizobuchi. "Identification and Sequence Analysis of Escherichia Coli Pure and Purk Genes Encoding 5'-Phosphoribosyl-5-Amino-4-Imidazole Carboxylase for De Novo Purine Biosynthesis." *JOURNAL OF BACTERIOLOGY*, (1989): 198-204.
7. Zengdao Chen, Jack E. Dixon, Howard Zalkin. "Cloning of a Chicken Liver Cdna Encoding 5-Aminoimidazole Ribonucleotide Carboxylase and 5-Aminoimidazole-4-Nsuccinocarboxamide Ribonucleotide Synthetase by Functional Complementation of Escherichia Coli Pur Mutants." *Proc. Natl. Acad. Sci. USA* 87, (1990): 3097-3101.



8. Maria V. Fawaz, Melissa E. Topper, Steven M. Firestine. "The Atp-Grasp Enzymes." *Bioorganic Chemistry*, (2011): 185–191.
9. Steven M. Firestine, Sing- Wing Poon, Ernest J. Mueller, JoAnne Stubbe and V. Jo Davisson. "Reaction Catalyzed by 5-Aminioimidazole Ribonucleotide Carboxylase from Escherichia Coli and Gallus Gallus : A Case for Divergent Catalytic Mechanisms?" *Biochemistry*, (1994): 11927-11934.
10. Ernest J. Mueller, Erik Meyer, Johannes Rudolph, V. Jo Davisson, and JoAnne Stubbe. "N5-Carboxyaminoimidazole Ribonucleotide: Evidence for a New Intermediate and Two New Enzymatic Activities in the De Novo Purine Biosynthetic Pathway of Escherichia Coli." *Biochemistry*, (1994): 2269-2278
11. Michael Taschner, Jerome Basquin, Christian Benda, and Esben Lorentzen. "Crystal Structure of the Invertebrate Bifunctional Purine Biosynthesis Enzyme Paics at 2.8 Å Resolution." *Protein*, (2013): 1473-1478.
12. Steven M. Firestine, V. Jo Davisson. "Carboxylases in De Novo Purine Biosynthesis. Characterization of the Gallusgallus Bifunctional Enzyme." *Biochemistry* 33, (1994): 11917-11926.
13. Firestine, Steven M., Shawn Misialek, Dena L. Toffaletti, Thomas J. Klem, John R. Perfect and V. Jo Davisson. "Biochemical Role of the Cryptococcus Neoformans Ade2 Protein in Fungal De Novo Purine

- Biosynthesis." *ARCHIVES OF BIOCHEMISTRY AND BIOPHYSICS* 351, (1998): 123-134.
14. Aaron A. Hoskins, Mariya Morar, T. Joseph Kappock, et al. "N<sup>5</sup>-Cair Mutase: Role of a Co<sub>2</sub> Binding Site and Substrate Movement in Catalysis." *Biochemistry* 45, (2007): 2842-2855.
  15. Irimpan I. Mathews, T. Joseph Kappock, JoAnne Stubbe, Steven E. Ealick. "Crystal Structure of Escherichia Colipure, an Unusual Mutase in the Purine Biosynthetic Pathway." *Structure*, (1999): 1395–1406.
  16. Sylvain Tranchimand, Courtney M. Starks, Irimpan I. Mathews, Susan C. Hockings, T. Joseph Kappock. "Treponema Denticola Pure Is a Bacterial Air Carboxylase." *Biochemistry*, (2011): 4623–4637.
  17. P. Brugarolas, E. M. Duguid, W. Zhang, C. B. Poor and C. He. "Structural and biochemical characterization of N<sup>5</sup>-carboxyaminoimidazole ribonucleotide synthetase and N<sup>5</sup>-carboxyaminoimidazole ribonucleotide mutase from Staphylococcus aureus." *Acta Crystallographica Section D: Biological Crystallography* 67 (2011): 707-715.
  18. Mahender B. Dewal, Steven M. Firestine. "Site-Directed Mutagenesis of Catalytic Residues in N<sup>5</sup>-Carboxyaminoimidazole Ribonucleotide Synthetase." *Biochemistry*, (2013): 6559–6567.
  19. Takagi, Hiroshi. "Protein Engineering of Subtilisin." *Biochemistry* 25, (1993): 307-312.

20. Sharon M. Kelly, Nicholas C. Price. "The Application of Circular Dichroism to Studies of Protein Folding and Unfolding." *Biochimica et Biophysica Acta* 1338, (1997): 161-185.
21. Greenfield, Norma J. "Using Circular Dichroism Spectra to Estimate Protein Secondary Structure." *Nature Protocol*, (2006): 2876-2890.
22. David L. Nelson, Albert L. Lehninger, Michael M. Cox. *Lehninger Principles of Biochemistry*. 2008.
23. Erik Meyer, T. Joseph Kappock, Chukwunenye Osuji, JoAnne Subbe. "Evidence for the Direct Transfer of the Carboxylate of N5-Carboxyaminoimidazole Ribonucleotide(N5-CAIR) to Generate 4-Carboxy-5-Aminoimidazole Ribonucleotide Catalyzed by Escherichia Coli Pure, and N5-Cair Mutase." *Biochemistry*, (1999): 3012-3018.
24. Price, Murray R. Badger and G. Dean. "The Role of Carbonic Anhydrase in Photosynthesis." *Annual Review of Plant Physiology and Plant Molecular Biology* 45, (1994): 369-392.
25. Xue Li, Qing-Chuan Zheng, Ji-Long Zhang, Hong-Xing Zhang. "Theoretical study on the mechanism of rearrangement reaction catalyzed by N5-carboxyaminoimidazole ribonucleotide mutase." *Computational and Theoretical Chemistry*, 2011: 77–82.
26. Ethan C. Settembre, Johnathan R. Chittuluru, Christopher P. Mill, T. Joseph Kappock and Steven E. Ealick. "Acidophilic Adaptations in the Structure of *Acetobacter Caeti* N5-Carboxylaminoimidazole

- Ribonucleotide Mutase (Pure)." *Acta Crystallographica Section D: Biological Crystallography* 60, (2004): 1753-1760.
27. Constantine, Charles M., Courtney M. Starks, Christopher P. Mill, Aaron E. Ransome, Steven J. Karpowicz, Julie A. Francois, Rena A. Goodman and T. Joseph Kappock. "Biochemical and Structure Studies of N5-Carboxyaminoimidazole Ribonucleotide Mutase from the Acidophilic Bacterium *Acetobacter Aceti*." *Biochemistry* 45, (2006): 8193-8208.
  28. Knowles, Jeremy R. "The Mechanism of Biotin-Dependent Enzymes." *Annual Review Biochemistry*, (1989): 195-221.
  29. Orlando Acevedo, William L. Jorgensen. "Medium effects on the decarboxylation of a biotin model in pure and mixed solvents from QM/MM simulations." *J. Org. Chem*, 2006: 4896–4902.
  30. Fischbach MA, Walsh C.T. "Antibiotics for emerging pathogens." *Science*, 2009: 1089-1093.
  31. Heather K. Allen, Justin Donato, Helena Huimi Wang, Karen A. Cloud-Hansen, Julian Davies, Jo Handelsman. "Call of the Wild: Antibiotic Resistance Genes in Natural Environments." *Nature Reviews Microbiology* 8, (2010): 251-259.
  32. Gerard D. Wrightemail, Hendrik Poinar. "Antibiotic Resistance Is Ancient: Implications for Drug Discovery." *Trends in Microbiology*, (2012): 157-159.

33. Steven M. Firestine, V. Jo Davisson. "A Tight Binding Inhibitor of 5-Aminoimidazole Ribonucleotide Carboxylase." *Journal of Medicinal Chemistry* 36, (1993): 3484–3486.
34. G. Sitta Sittampalam, Steven D Kahl, William P Janzen. "High-Throughput Screening: Advances in Assay Technologies " *Current Opinion in Chemical Biology*, (1997): 384-391.
35. Carnero, Amancio. "High Throughput Screening in Drug Discovery." *Clinical and Translational Oncology* 8, no. 7 (2006): 482-490.
36. Fawaz, Maria V. *Novel Inhibitors of the Bacterial De Novo Purine Biosynthesis Enzymes, N5-Carboxyaminoimidazole Ribonucleotide Synthetase and Mutase*. 2012.
37. Michael W. Pantoliano, Eugene C. Petrella, Joseph D. Kwasnoski, Victor S. Lobanov, James Myslik, Edward Graf, Ted Carver, Eric Asel, Barry A. Springer, Pamela Lane and F. R. Salemme. "High-Density Miniaturized Thermal Shift Assays as a General Strategy for Drug Discovery." *Journal of Biomolecular Screening*, (2001): 429-440.
38. Maxwell D. Cummings, Michael A. Farnum. and Marina I. Nelen. "Universal Screening Methods and Application of Thermofluor." *Journal of Biomolecular Screening*, (2006): 854-863
39. Frank H Niesen, Helena Berglund, Masoud Vedadi. "The Use of Differential Scanning Fluorimetry to Detect Ligand Interactions That Promote Protein Stability." *Nature Protocol* (2007): 2212-2221.

40. Tian Zhu, Hyun Lee, Hao Lei, Christopher Jones, Kavankumar Patel, Michael E. Johnson, and Kirk E. Hevener. "Fragment-Based Drug Discovery Using a Multidomain, Parallel Md-Mm/Pbsa Screening Protocol." *Journal of Chemical Information and Modeling*, (2013): 560-572.
41. Kelly L. Sullivan, Ioredana C. Huma, Elwood A. Mullins, Michael E. Johnson, T. Joseph Kappock. "Metal Stopping Reagents Facilitate Discontinuous Activity Assays of the De Novo Purine Biosynthesis Enzyme PurE." *Analytical Biochemistry* (2014): 43-45.
42. Jane C. Andrews, John P. Nolan, Roy H. Hammerstedt, and Barry D. Bavister. "Characterization of N-(6-Methoxy-8-Quinolyloxy)-P-Toluenesulfonamide for the Detection of Zinc in Living Sperm Cells." *Cytometry* 21, (1995): 153-159.
43. Jeffrey W. Meeusen, Henry Tomaszewicz, Andrew Nowakowski and David H. Peterin. "Tsq (6-Methoxy-8-P-Toluenesulfonamido-Quinoline), a Common Fluorescent Sensor for Cellular Zinc, Images Zinc Proteins." *Inorganic Chemistry*, (2011): 7563-7573.
44. Nimmo, Alan G.S. Robertson and Hugh G. "Site-Directed Mutagenesis of Cysteine-195 in Isocitrate Lyase from *Escherichia coli* M1308." *Biochemistry. J.* 305, (1995): 239-244.
45. Steven M. Firestine, Hanumantharao Paritala, Jane E. McDonnell, James B. Thoden, Hazel M. Holden. "Identification of Inhibitors of N<sup>5</sup>-

Carboxyaminoimidazole Ribonucleotide Synthetase by High-Throughput Screening." *Bioorganic & Medicinal Chemistry* 17, (2009): 3317–3323.

**ABSTRACT****Site-Directed Mutagenesis of Conserved Amino Acids Residues in N<sup>5</sup>-  
Carboxyaminoimidazole Ribonucleotide Mutase  
&  
Developing a High-Throughput Screen Assay for the Discovery of N<sup>5</sup>-  
Carboxyaminoimidazole Ribonucleotide Mutase Inhibitors**

by

**ZHIWEN SHI****July 2014****Advisor:** Dr. Steven M. Firestine**Major:** Pharmaceutical Sciences**Degree:** Master of Science

The *de novo* purine biosynthesis pathway plays a critical role in providing new purines to the cell. Previous studies have shown differences between the human and bacterial pathways which suggests that pathway may be a potential target for antibiotic drug discovery. Three critical enzymes are involved in the pathway divergence. In the bacterial pathway, N<sup>5</sup>-CAIR synthetase (PurK) first converts AIR to N<sup>5</sup>-CAIR, which is then transformed into CAIR catalyzed by the enzyme N<sup>5</sup>-CAIR mutase (Class I PurE). In the human pathway, AIR carboxylase (Class II PurE) catalyzes the direct conversion of AIR to CAIR. Class I and Class II PurEs have structure and sequence similarities but also are functionally different. However, the residues responsible for these differences are unknown. In this study, we hypothesized that the class-specific conserved residues in the active site might be the key to



determining the functional differences between the two PurEs. Site-directed mutagenesis was used to convert residues of Class I PurEs to Class II PurEs. Several mutant PurEs were made and examined for CO<sub>2</sub>-dependent conversion of AIR to CAIR. Two mutants H71A and H71G displayed CO<sub>2</sub> dependent that was similar to that observed for AIR carboxylase. Additional studies revealed that these enzymes also were capable of using N<sup>5</sup>-CAIR as a substrate. This indicates that the H71A and H71G mutant have AIR carboxylase as well as N<sup>5</sup>-CAIR mutase activity. Examination of the crystal structure of N<sup>5</sup>-CAIR mutase indicates that His71 is at the bottom of the active site and removal of this residue creates a channel between active sites in two subunits. We speculate that this channel may be key for the utilization of CO<sub>2</sub>.

The second project focused on developing an appropriate high-throughput screening (HTS) assay for Class I PurE inhibitor. Existing assays have significant issue for HTS. We examined both a thermo shift assay as well as a metal stopping/fluorescence assay. While both assays had some potential issues for analysis indicated that neither assay was suitable for HTS.

## **AUTOBIOGRAPHICAL STATEMENT**

### **EDUCATION**

2012-2014 M.S. Pharmaceutical Sciences, Wayne State University, Michigan

2007-2011 B.S. Pharmacy, Zhejiang Chinese Medical University, China

### **PROJECTS**

1. Site-Directed Mutagenesis of Conserved Amino Acids Residues in N<sup>5</sup>-Carboxyaminoimidazole Ribonucleotide Mutase: converting N<sup>5</sup>-CAIR mutase into Aminoimidazole Ribonucleotide carboxylase
2. Developing a High-Throughput Screening Assay for the Discovery of N<sup>5</sup>-Carboxyaminoimidazole Ribonucleotide Mutase Inhibitors